Resource

Cell Reports

Genome-wide RNAi Screen Identifies Networks Involved in Intestinal Stem Cell Regulation in *Drosophila*

Graphical Abstract

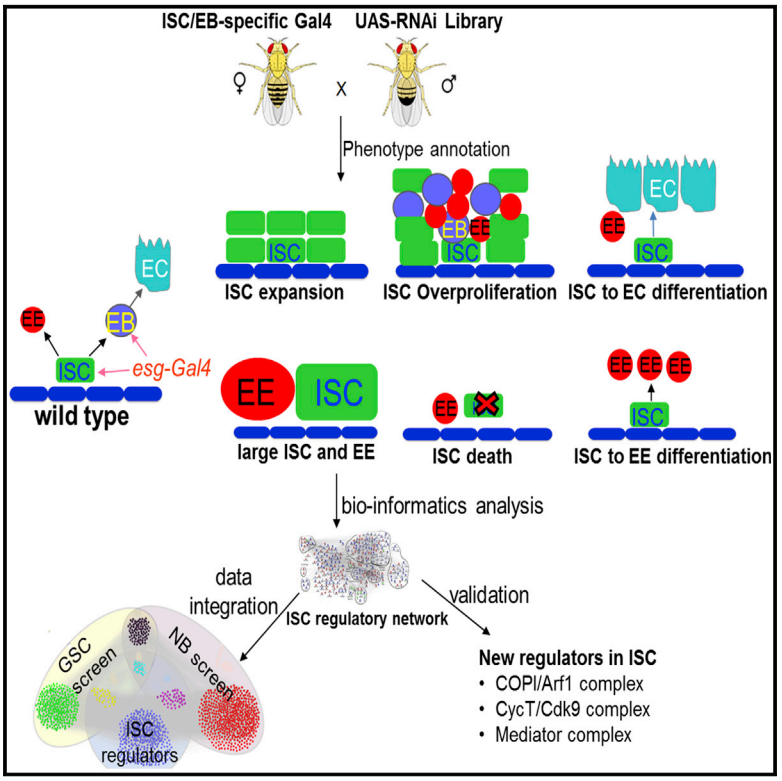

Highlights

- Genome-wide RNAi screen identifies 405 genes required for ISC maintenance
- Comparison of ISC with female GSCs, and NBs finds common and distinct regulators
- COPI/Arf79F, CycT/Cdk9, and Mediator complexes are required in ISCs
- Unique cell-cycle regulators maintain diploid cells in intestine

Authors

Xiankun Zeng, Lili Han, ..., Xinhua Lin, Steven X. Hou

Correspondence

hous@mail.nih.gov

In Brief

In this study, Zeng et al. perform a systematic genome-wide RNAi screen and identify genes that regulate intestinal stem cells in *Drosophila*. These data provide a useful resource for understanding the regulatory networks of self-renewal and differentiation of adult somatic stem cells.

Zeng et al., 2015, Cell Reports *10*, 1226–1238
February 24, 2015 ©2015 The Authors
http://dx.doi.org/10.1016/j.celrep.2015.01.051

OPEN ACCESS
CellPress

Cell Reports
Resource

Genome-wide RNAi Screen Identifies Networks Involved in Intestinal Stem Cell Regulation in *Drosophila*

Xiankun Zeng,[1] Lili Han,[2] Shree Ram Singh,[1] Hanhan Liu,[1] Ralph A. Neumüller,[4,5] Dong Yan,[4] Yanhui Hu,[4] Ying Liu,[1] Wei Liu,[1] Xinhua Lin,[2,3] and Steven X. Hou[1,*]

[1]Basic Research Laboratory, National Cancer Institute at Frederick, NIH, Frederick, MD 21702, USA
[2]Key Laboratory of Stem Cell and Developmental Biology, Institute of Zoology, Chinese Academy of Sciences, Beijing 100864, China
[3]Division of Developmental Biology, Cincinnati Children's Hospital Medical Center, Cincinnati, OH 45229, USA
[4]Department of Genetics, Harvard Medical School, Boston, MA 02115, USA
[5]Gene Center and Department of Biochemistry, Ludwig-Maximilians-Universität, Feodor-Lynen-Strasse 25, 81377 München, Germany
*Correspondence: hous@mail.nih.gov
http://dx.doi.org/10.1016/j.celrep.2015.01.051

SUMMARY

The intestinal epithelium is the most rapidly self-renewing tissue in adult animals and maintained by intestinal stem cells (ISCs) in both *Drosophila* and mammals. To comprehensively identify genes and pathways that regulate ISC fates, we performed a genome-wide transgenic RNAi screen in adult *Drosophila* intestine and identified 405 genes that regulate ISC maintenance and lineage-specific differentiation. By integrating these genes into publicly available interaction databases, we further developed functional networks that regulate ISC self-renewal, ISC proliferation, ISC maintenance of diploid status, ISC survival, ISC-to-enterocyte (EC) lineage differentiation, and ISC-to-enteroendocrine (EE) lineage differentiation. By comparing regulators among ISCs, female germline stem cells, and neural stem cells, we found that factors related to basic stem cell cellular processes are commonly required in all stem cells, and stem-cell-specific, niche-related signals are required only in the unique stem cell type. Our findings provide valuable insights into stem cell maintenance and lineage-specific differentiation.

INTRODUCTION

Animal tissues and organs are generated and maintained by stem cells. During development, they generate most of the cell types to form an organ, while in adult animals, they maintain tissue homeostasis by supplying new cells to replace dying or damaged ones. To accomplish this task, stem cells have to continuously renew themselves and, at the same time, generate daughter cells to produce terminal differentiated cells for their organ-specific functions. Furthermore, the somatic differentiated cells can be reprogrammed into induced pluripotent stem cells (iPSCs) through overexpression of a few transcription factors (TFs) or the metabolic switch (Ito and Suda, 2014; Takahashi and Yamanaka, 2006; Zhang et al., 2012). The primary functions of activated oncogenes and inactivated tumor suppressors may be to reprogram cellular metabolism and convert somatic cancer cells into pluripotent tumor-initiating cells (also called cancer stem cells [CSCs]) (Ward and Thompson, 2012; Zhang et al., 2012). Therefore, understanding how adult stem cells (particularly, somatic adult stem cells) are regulated is important for understanding tissue degeneration and tumorigenesis.

Because the digestive organs are the fastest renewing organs in all animals (Hakim et al., 2010), intestinal stem cells (ISCs) in both adult mouse and *Drosophila* have been studied extensively. *Drosophila* ISCs divide asymmetrically to produce one new ISC (self-renewal) and one immature enteroblast (EB) or one pre-enteroendocrine (pre-EE) cell. The EB differentiates into an absorptive enterocyte (EC), and the pre-EE cell matures into a secretory EE cell (Biteau and Jasper, 2014; Micchelli and Perrimon, 2006; Ohlstein and Spradling, 2006; Zeng and Hou, 2015). Notch (N) signaling plays a major role in regulating ISC self-renewal and differentiation (Micchelli and Perrimon, 2006; Ohlstein and Spradling, 2006, 2007).

These different cell types can be identified morphologically as well as by their expression of marker genes. ISCs are diploid, have a small nucleus, and express Delta (Dl), a ligand for the N receptor signal transduction pathway. EBs are diploid, have a small nucleus, and express *Su(H)GBE-lacZ*, a transcriptional reporter of the N pathway. ECs are polyploid, have a large nucleus, and express the transcriptional factor Pdm1. EE cells are diploid, have a small nucleus, and express the transcription factor Prospero (Pros). Like mammalian intestinal epithelium, the *Drosophila* intestinal epithelium is also constantly undergo turnover and can regenerate after tissue damage (Amcheslavsky et al., 2009; Jiang et al., 2009; reviewed in Jiang and Edgar, 2011).

However, a systematic molecular understanding of self-renewal and lineage-specific differentiation of adult somatic stem cells is still lacking. In mammals, lists of stem-cell-enriched genes have been identified in both mouse ISCs and hair follicle stem cells through combined transcriptomics and proteomics (Morris et al., 2004; Muñoz et al., 2012; Tumbar et al., 2004). However, the

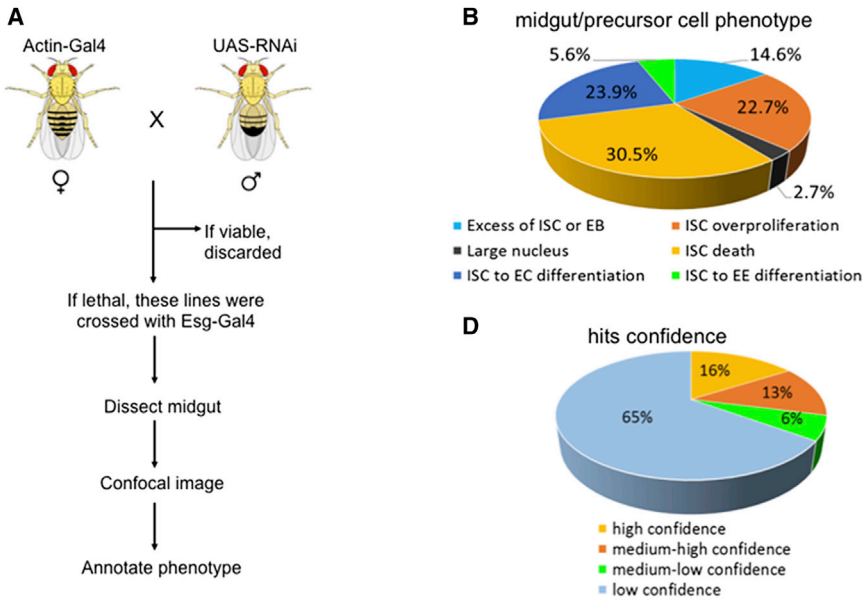

C

Vector	Fly lines	Midgut/precursor cell phenotype	Percentage	RNAi
VDRC	6027	340	5.64	dsRNA
VALIUM1	49	10	20.40	dsRNA
VALIUM10	706	57	8.07	dsRNA
VALIUM20	658	64	9.72	shRNA
NON-VALIUM	38	7	18.42	dsRNA

Figure 1. Transgenic RNAi Screen

(A) Workflow of the ISC RNAi screen.

(B) The *esg*^{ts} > *RNAi* female flies were dissected after 7 days at 29°C. Their posterior midguts were stained with antibodies and analyzed by confocal microscopy. The phenotypes were divided into six categories.

(C) Summary of the screen results.

(D) Confidence of identified 405 genes from the screen. High-confidence genes are identified by two or more independent RNAi lines. Medium-high-confidence genes are identified by one RNAi line, but they cocomplex with high-confidence hits. Medium-low-confidence genes are identified by one RNAi line, but they cocomplex with other low-confidence hits. Low-confidence hits are identified by one RNAi only.

See also Tables S1, S2, S3, S4, and S5.

functional relevance of these genes is largely unknown. Recent developments in genome-wide RNAi techniques in *Drosophila* have enabled the knockdown of near-complete sets of genes involved in cellular processes in living animals (Dietzl et al., 2007; Ni et al., 2011). In addition, genome-wide RNAi screens have been performed to identify regulatory networks function in several somatic tissues, including stem cells (Baumbach et al., 2014; Berns et al., 2014; Neely et al., 2010; Neumüller et al., 2011; Schnorrer et al., 2010; Yan et al., 2014). In this study, we carried out a genome-wide RNAi screen for genes that regulate ISC fates. We identified 405 genes that regulate ISC self-renewal, ISC proliferation, ISC-to-EC differentiation, ISC-to-EE cell differentiation, and ISC survival. Cross-correlation with regulators, neuroblasts (Nbs), and female germline stem cells (GSCs) revealed ISC-specific as well as shared regulators of the stem cells. Our data provide a useful resource for dissecting the regulatory networks of self-renewal and differentiation of adult somatic stem cells.

RESULTS

Test Conditions for High-Throughput Screen of Genes Involved in ISC Regulation

To identify candidate genes involved in ISC regulation, we generated GFP-marked cells that expressed *UAS-RNAi* in adult *Drosophila* intestine using *esg-Gal4, UAS-GFP/+; tub-Gal80*^{ts}*/+* driver. In the midgut, *esg-Gal4* is mainly expressed in the ISCs and EBs (Micchelli and Perrimon, 2006). The temperature-sensitive Gal80 inhibitor, *Gal80*^{ts} (McGuire et al., 2003), suppresses *esg-Gal4* activity at the permissive temperature (18°C). When cultured at 18°C, these flies grew to adulthood with no obvious phenotype and no GFP expression (data not shown). We then shifted the adult flies to the restrictive temperature (29°C). After 1 week, the flies were dissected and examined under confocal microscope for ISC phenotypes.

The RNAi methodology has certain restrictions (Dietzl et al., 2007; Ni et al., 2011). First, the P-element-based upstream activating sequence (UAS)-hairpin constructs are randomly integrated in the genome, and the level of hairpin expression is affected by its chromosomal location. Second, the RNA level can be reduced only to a variable degree by the RNAi-mediated knockdown, which, in some cases, may insignificantly affect the gene's activity. In addition, there are a large number of nonessential genes whose null mutations have no phenotype (flybase). To reduce the overall false-negative rate and conduct an efficient screen, we first performed a pilot experiment in which we selected 2,000 RNAi lines at random. Each of these lines was crossed in duplicate to *Act5C-Gal4* and to *esg-Gal4, UAS-GFP/+; tub-Gal80*^{ts}*/+* drivers. The progeny from the cross with *Act5C-Gal4* was screened for lethality and any visible adult phenotype. The progeny from the cross with *esg-Gal4, UAS-GFP/+; tub-Gal80*^{ts}*/+* was scored for ISC phenotype. We found that 95.4% of RNAi lines with ISC phenotypes were lethal in the cross with *Act5C-Gal4.* In the following screen, we first crossed all RNAi lines with *Act5C-Gal4* to test lethality and then only crossed the lethal lines with *esg-Gal4, UAS-GFP/+; tub-Gal80*^{ts}*/+* to screen ISC phenotype (Figure 1A).

Genome-wide RNAi Screen for ISC Phenotype in Adult *Drosophila*

In total, we screened 16,562 transgenic lines of either double-stranded RNA (dsRNA) or short, small hairpin RNA (shRNA) from both the Vienna *Drosophila* RNAi Center (VDRC) and

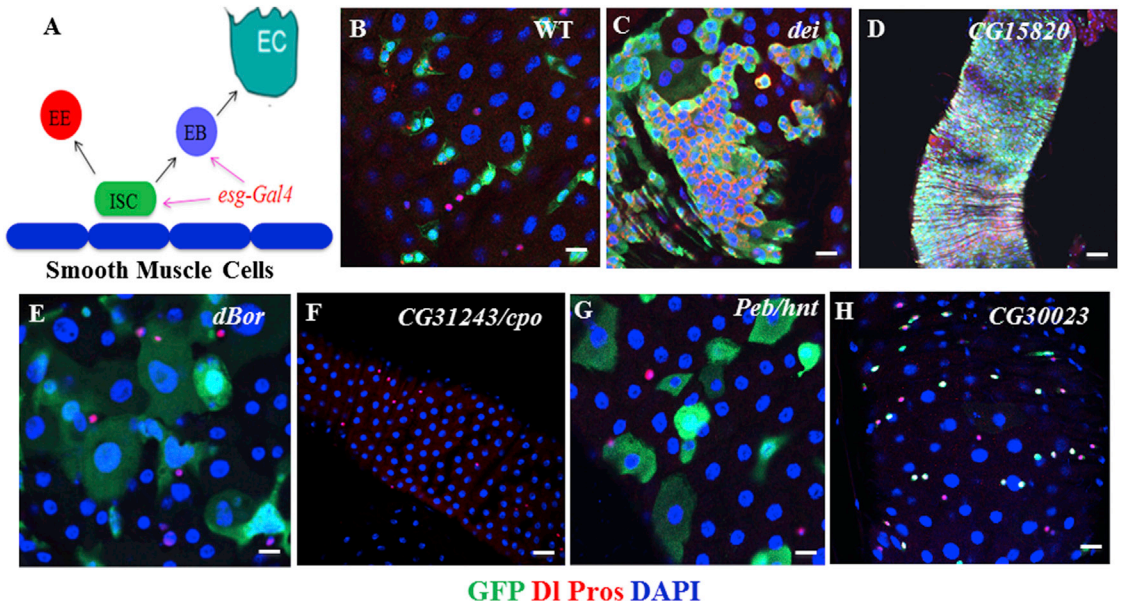

Figure 2. Representative Phenotypes Identified in the RNAi Screen

(A) Diagram of ISC lineage and expression of *esg-Gal4* used in the screen.
(B) Wild-type (WT) control.
(C) Knockdown of *dei* resulted in ISC expansion.
(D) Knockdown of *CG15820* resulted in ISC overproliferation.
(E) Knockdown of *dBor* resulted in large nuclei.
(F) Knockdown of *cpo* resulted in ISC death.
(G) Knockdown of *Peb/hnt* resulted in ISC-to-EC differentiation.
(H) Knockdown of *CG30023* resulted in ISC-to-EE cell differentiation.
The posterior midguts of corresponding flies were dissected, stained with antibodies of GFP+Dl+Pros+DAPI, and analyzed by confocal microscopy. Scale bars represent 5 μm (B, C, E, G, and H) and 10 μm (D and F).
See also Figure S2 and Tables S1A and S1C–S1E.

Bloomington stock centers (Figure 1C; Table S5), representing 12,705 of the 14,139 protein-coding genes (89.8%) in release 5.7 of the *Drosophila* genome (Wilson et al., 2008). Among the total 16,562 transgenic lines tested, 7,429 (44.8%) lines corresponding to 6,170 genes were lethal once expressed by the Act5C-Gal4 driver.

We then expressed the 7,429 transgenic lines in ISCs and EBs by crossing each line with *esg-Gal4, UAS-GFP/+; tub-Gal80^{ts}/+* (Figure 2A) and analyzed 5–10 flies each for ISC phenotypes by observing the number of GFP-positive cells in midguts. A total of 478 promising lines, which correspond to 405 genes, were scored (Figure 1C) from the first-round screen were repeatedly screened and stained with molecular markers to confirm the phenotypes.

Quality Evaluation

Six lines of evidence suggest that our screen has identified ISC regulators with high confidence. First, the N signal transduction pathway plays a major role in regulating ISC-to-EC differentiation; inactivation of the pathway resulted in an excess of ISCs, and activation of the pathway resulted in premature ISC-to-EC differentiation (Bardin et al., 2010; Beebe et al., 2010; Micchelli and Perrimon, 2006; Ohlstein and Spradling, 2006, 2007; Perdigoto et al., 2011). In this screen, we identified 19 positive regulators in the N pathway whose knockdowns resulted in an excess of ISCs or EBs and eight negative regulators of the N pathway whose knockdowns resulted in premature ISC-to-EC differentiation (Table S1). Second, we found many previously identified genes regulating ISC functions (Table S1). Third, many of the identified hits (132 genes) whose products are components of protein complexes show a high degree of phenotypic similarity (Figure 1D; Tables S3 and S4). Fourth, of 405 genes identified, 310 genes were from VDRC lines; among them, we randomly verified 65 genes by at least two or more independent lines (Figure 1D; Tables S4 and S5), and the rest of the lines scored were from either GD or KK libraries with no off-targets, as shown on the VDRC website. Among 405 genes, 95 genes were from Bloomington lines, which were predicted to have no off-targets. Furthermore, we also verified some of the genes identified in the RNAi screen by mutant clone analysis. Furthermore, even though many of the GSC-specific genes were lethal in the primary screen, none of them show any phenotypes in ISCs. Together, these lines of evidence suggest that our screen has a very low percentage (~5%) of off-targets. Fifth, among the remaining low-confidence genes, nine [*eIF-5*, *l(1)10Bb*, *cas*, *ial/AurB*, *dia*, *pAbp*, *Ccn*, *Crn*, and *CSN8*] were identified in all three stem cell RNAi screens (Nbs: Neumüller et al., 2011; female GSC: Yan et al., 2014; Tables S4 and S5), and 42 other genes

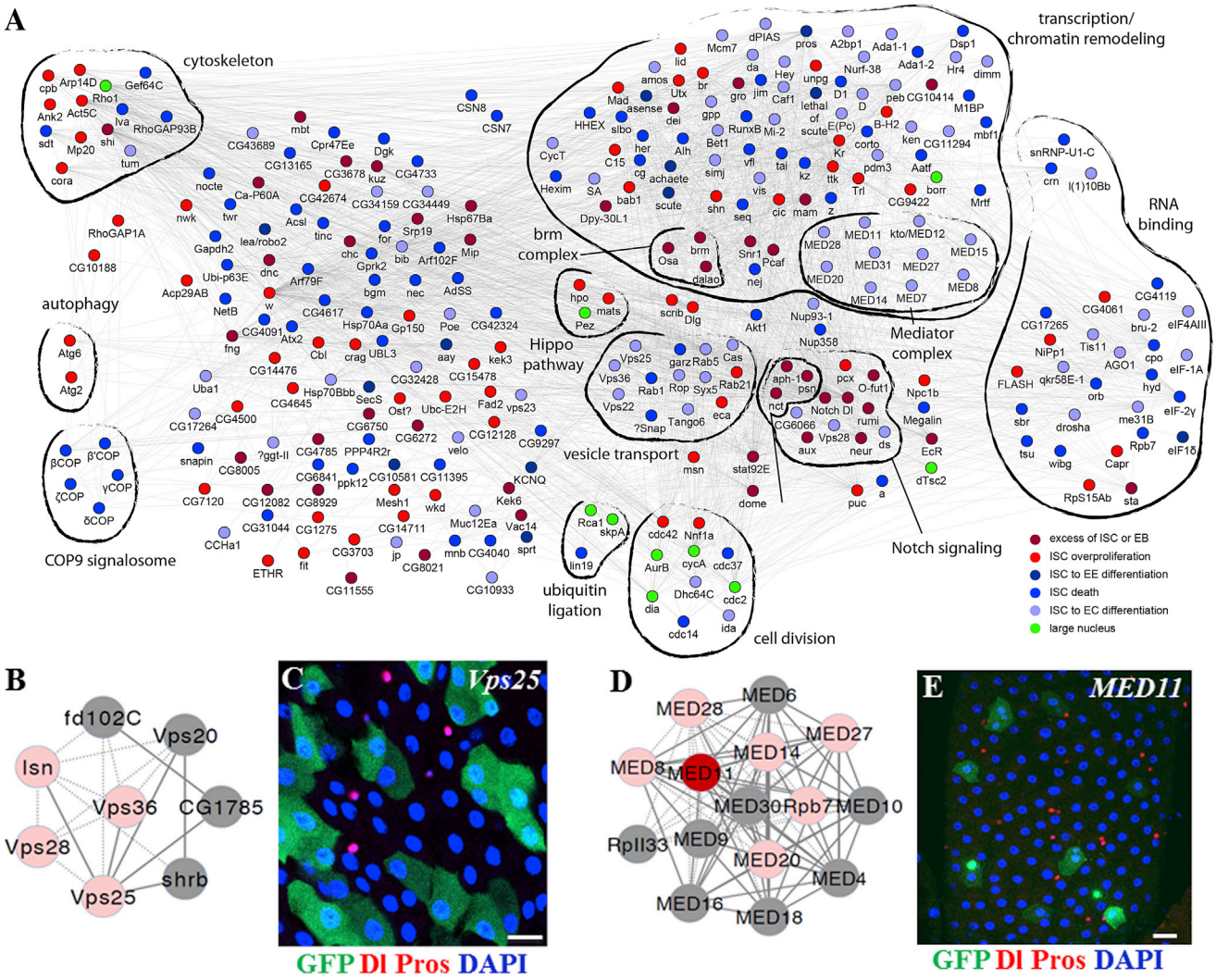

Figure 3. Regulatory Network for Genes Identified from the Screen

(A) Network of genes identified in the ISC screen. Genes are shown as nodes, and the node colors indicate the observed phenotype in the screen. The edges denote the interactions among the nodes. The distinct molecular complexes are outlined by thick black lines. Red and blue represent genes identified in the screen, and gray represents genes that are not identified in the screen but were identified by querying publicly available databases.

(B) Diagram of the endosome complex.

(C) Knockdown of *Vps25* resulted in ISC-to-EC differentiation.

(D) Diagram of the mediator complex.

(E) Knockdown of *MED11* resulted in ISC-to-EC differentiation.

Scale bars represent 5 μm (C and E).

See also Figure S1.

were identified in two of the three stem cell RNAi screens (Table S4). Finally, we showed efficient knockdown of a select set of genes by qPCR analysis or antibody staining (Table S2).

Gene Network that Regulates ISC Fates

To better analyze our screen results, we generated a gene-interaction network by querying publicly available databases containing yeast two-hybrid interactions, protein-protein interactions, text-mining data, and genetic interactions between *Drosophila* genes (Figure 3A). We divided the phenotypes into six categories: (1) genes whose knockdown resulted in an excess of ISCs or EBs; (2) genes important for ISC proliferation; (3) genes important for ISCs to maintain diploid status; (4) genes important for ISC survival; (5) genes important for ISC-to-EC differentiation; and (6) genes important for ISC-to-EE cell differentiation (Figures 1B and 2B–2H; Table S1). We performed a complex-enrichment analysis using COMPLEAT (Vinayagam et al., 2013) and identified a number of protein complexes required for ISC fate determination (Figures 3 and S1).

Genes Whose Knockdown Resulted in an Excess of ISCs or EBs

RNAi-mediated knockdowns of genes required for ISC or EB differentiation resulted in the accumulation of undifferentiated *esg*+ diploid cells. From our phenotype and network analysis, we identified three unique phenotypes that disrupt ISC differentiation; each phenotype involves genes that function in a distinguishing protein complex or pathway.

The Classic N-Signaling Network

RNAi-mediated knockdowns of genes in the N-signaling network resulted in either expansion of both ISCs and EE cells (Dl high and EE cells more) (Table S1A) or expansion of ISCs only (Dl high and EE normal; Figure 2C; Table S1A). Among known components of the N pathway (Bray, 2006; Fortini, 2009; Guruharsha et al., 2012), we found that knockdowns of *N*, *O-fut1*, *rumi*, *kuz*, *psn*, *neur*, *shi*, *nct*, *aux*, *Ca-P60A*, and *mam* resulted in expansion of both ISCs and EEs (Dl high and EE cells more) (Table S1A), while knockdowns of *aph-1*, *chc*, and *dei* resulted in expansion of only ISCs (Dl high and EE cells normal) (Figure 2C; Table S1A). Among the five new components of the N pathway identified in a previous genome-wide RNAi screen (Mummery-Widmer et al., 2009), knockdowns of CG34345 and CG8021 resulted in expansion of both ISCs and EE cells, while knockdowns of CG5608 (Vac14), CG8136, and CG11286 resulted in expansion of only ISCs (Table S1A). These results suggest that components in the N pathway have differential requirements in ISC and EE fate regulation.

In addition to the reported components in the N-signaling network, we identified 26 other genes whose knockdowns resulted in expansion of ISCs (Table S1A). Among them are a histone acetyltransferase ATAC2 and a protein phosphatase type 2A (PP2A) regulator (*dPR72*, CG4733). Knockdown of ATAC2 resulted in dramatic accumulation of Dl and expansion of ISCs without affecting EE cells (Ma et al., 2013; Table S1A). PP2A was reported to be a brain tumor suppressor that can inhibit self-renewal of Nbs (Wang et al., 2009). Knockdowns of the remaining 24 genes resulted in either expansion of both ISCs and EE cells or expansion of ISCs only (Table S1A). Further investigations of these genes will significantly advance our knowledge of ISC self-renewal/differentiation and the N-signaling network.

The Osa Complex

RNAi knockdowns of genes in the Osa-containing SWI/SNF chromatin-remodeling complex resulted in ISC expansion and EE cell reduction. In this screen, we identified four components of the SWI/SNF complex: *osa*, *snr1*, *brm*, and *dalao* (Table S1A). However, these ISCs express low levels of Dl but high levels of another ISC marker, Sanpado (Spno) (Table S1A) (Zeng et al., 2013). In a recent publication (Zeng et al., 2013), we demonstrated that the OSA-containing SWI/SNF chromatin-remodeling complex regulates ISC-to-EC lineage differentiation by controlling *Dl* transcription and EE cell lineage differentiation by controlling *ase* transcription.

In addition to the components in the SWI/SNF chromatin-remodeling complex, we identified eight other genes whose knockdowns resulted in ISC expansion and EE cell reduction (Table S1A). Further investigations of these genes will advance our knowledge of *Dl* and *ase* regulations.

The JAK-STAT Pathway

RNAi-mediated knockdowns of both *dome* and *stat92E* resulted in EB accumulation (Table S1A); the GFP+ cells were Dl− Pros−. This finding is consistent with previous reports that mutations in the JAK-STAT signal transduction pathway disrupted EB differentiation (Beebe et al., 2010; Jiang et al., 2009).

Genes Important for ISC Proliferation

RNAi-mediated knockdowns of genes negatively regulating ISC proliferation resulted in hyperplasia, a dramatic increase of both ISCs and their differentiated cells (Figure 2D). From our phenotype and network analysis, we identified components in five known pathways, three novel complexes, and many other novel genes whose RNAi-mediated knockdowns resulted in midgut hyperplasia. Among the known pathways, we identified five negative regulators (*Cbl*, *Kek3*, *ttk*, *Cic*, and *CG15528*) in the epidermal growth factor receptor (EGFR)/mitogen-activated protein kinase (MAPK) signal transduction pathway (Table S1B). EGFR/Ras/MAPK signaling plays a major role in ISC proliferation (Biteau and Jasper, 2011; Jiang et al., 2011; Xu et al., 2011); two components in the Dpp signaling pathway (Mad and Shn) negatively regulate *Drosophila* midgut homeostasis (Guo et al., 2013). In mouse intestine, EGFR signaling positively and bone morphogenetic protein (BMP) signaling negatively regulate stem cell proliferation (reviewed in Clevers, 2013). Therefore, the functions of the EGFR and Dpp/BMP in ISCs are conserved in *Drosophila* and mouse. We also identified a negative regulator (*puc*) of the JNK pathway, which also regulates ISC proliferation and differentiation (Biteau et al., 2008; Hochmuth et al., 2011); three components of the Hippo pathway (*hpo*, *mats,* and *msn*), which negatively regulates ISC proliferation (Li et al., 2014; Karpowicz et al., 2010; Ren et al., 2010; Staley and Irvine, 2010); and two components in the Scrib/Dlg tumor suppressor pathway (*dlg* and *scrib*), indicating that the Scrib/Dlg pathway also negatively regulates ISC proliferation.

In addition to the classic pathways, we identified three components in the magnesium transporter complex (CG7830, CG15168, and CG11781), two components in the aminopeptidase complex (CG6372 and CG4439), and two components in the autophagosome (Atg2 and Atg6) whose knockdowns resulted in midgut hyperplasia.

We also identified 73 other genes (Table S1B) whose RNAi-mediated knockdowns resulted in midgut hyperplasia. The information provides a rich resource for investigating ISC proliferation and midgut hyperplasia in future studies.

Genes Necessary for the Maintenance of ISCs' Diploid Status

In this screen, we identified 11 genes whose RNAi-mediated knockdowns resulted in GFP+ cells with much larger nuclei (Figure 2E; Figures 4A–4F; Table S1C), including *TSC2*. It was previously reported that TSC1/2 and Myc coordinately regulate ISC growth and division in the *Drosophila* posterior midgut (Amcheslavsky et al., 2011). In *TSC2* dsRNA-expressing guts, the size of the ISCs, but not ECs or EE cells, increased by ~10-fold in 10 days after RNAi initiation. The mutant ISCs expressed the ISC marker Dl but are nonfunctional because they can no longer divide or differentiate (Amcheslavsky et al., 2011). In normal

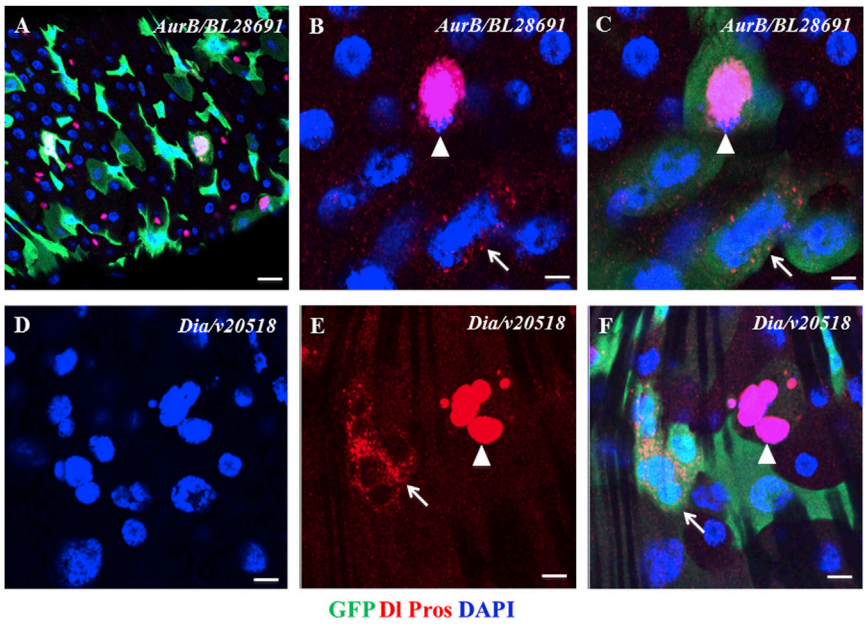

Figure 4. The Larger Nuclei of Knockdowns of *AurB* and *Dia*

(A–C) Knockdown of *AurB* resulted in larger nuclei of ISCs (arrows in B and C) and EE cells (arrowheads in B and C).

(D–F) Knockdown of *Dia* resulted in larger nuclei of the ISC cluster (arrows in E and F) and the EE cell cluster (arrowheads in E and F).

The posterior midguts of corresponding flies were dissected, stained with antibodies of GFP+Dl+Pros+DAPI, and analyzed by confocal microscopy. Scale bars represent 10 μm (A), 2.5 μm (B and C), and 5 μm (D–F).

See also Table S1C.

development and adult tissue homeostasis, cells' growth and division are precisely monitored by the checkpoint controls. Cells will divide to maintain the original cell size once they grow in size by approximately 2-fold. Adult midgut ISCs have a slower intrinsic cell cycle (>24 hr) (Micchelli and Perrimon, 2006; Ohlstein and Spradling, 2006) and differences in checkpoint controls, which may allow the excessive growth to take place in *TSC2* dsRNA-expressing cells until the growth passes a critical point that blocks division (Amcheslavsky et al., 2011).

Consistent with the aforementioned hypothesis, of the 11 genes identified in our screen, 8 (*CG10800/Rca1*, *CG4454/borr*, *CG8214/Cep89*, *CG16983/skpA*, *CG5363/cdc2*, *CG5960/cycA*, *CG6620/ial/AurB*, and *CG1768/dia*) regulate mitotic cell cycle or mitotic cytokinesis. Knockdowns of these genes might block mitotic cell division and allow excessive cell growth. However, we found that, unlike the phenotypes of the published *TSC2* dsRNA-expressing cells, some of the GFP+ cells with larger nuclei expressed the EE cell marker Pros (Figures 4A–4F), and we even identified a cluster of EE cells with larger nuclei in the *dia* dsRNA-expressing gut (Figures 4E and 4F, arrowheads). These data suggest that excessive DNA amplification and cell growth can happen in both diploid ISCs and EE cells. The data from this screen provide a useful resource for investigating the regulation of the adult stem cell cycle, DNA amplification, and cell growth.

Genes Important for ISC Survival

In this screen, we identified 124 genes whose RNAi-mediated knockdowns resulted in ISC death (Figures 2F, S2C, and S2D; Table S1D).

The COPI Complex and Lipolysis

Among the genes that are required for ISC survival, we identified seven components in the coat protein complex I (COPI)/Arf1 (Arf79F) complex (Figures S2C and S2D; Table S1D), including Arf79F, Garz (guanine nucleotide exchange factor of Arf79F), and several components of the vesicle-mediated COPI transport complex (ζCOP, βCOP, β'COP, γCOP, and δCOP) (Figures S2C and S2D; Table S1D). The phenotypes of ζCOP, βCOP, δCOP, and Arf79F were confirmed by using three independent dsRNA or shRNA lines for each gene (Table S1D). The cell survival function of these genes was stem cell specific, because knockdowns of these genes in ECs using NP1-Gal4 did not result in EC death (compare Figure S2F with Figure S2E; data not shown).

COPI and coat protein complex II (COPII) are essential components of the trafficking machinery for vesicle transportation between the ER and Golgi (reviewed in Lee et al., 2004). The COPII complex mediates vesicle cargo transport from the ER to the Golgi, while the COPI complex mediates cargo transport from the Golgi back to the ER. In addition to its trafficking function, the COPI complex regulates lipid droplet utilization (lipolysis) by transporting enzymes of lipolysis to the lipid droplet surface (Beller et al., 2008; Soni et al., 2009). In this screen, we did not identify any components in the COPII complex, suggesting that lipolysis, rather than the general trafficking machinery between the ER and the Golgi, is required for stem cell survival. Consistent with this hypothesis, we also identified acyl-coenzyme A (CoA) synthetase long-chain (ACSL), an enzyme in the *Drosophila* lipolysis/β-oxidation pathway (Zhang et al., 2009; Palanker et al., 2009), and bubblegum (bgm), a very-long-chain fatty acid-CoA ligase activity (Min and Benzer, 1999).

In addition, we identified 113 other genes whose RNAi-mediated knockdowns resulted in ISC death (Table S1D). The data provide a rich resource for investigating the molecular mechanisms that specifically regulate stem cell death and survival.

The CycT/Cdk9 Complex

We also identified the *Drosophila Cyclin T* (*CycT*) gene (Figure 5A). Knockdowns of *CycT* by two independent dsRNAs (V37562 and BL31762) and two independent shRNAs (BL32976 and BL35168) all resulted in the ISC quiescence/death phenotype (compare Figure 5C with Figure 5B; Table S1D). Midguts of *CycT* knockdown contain single and isolated GFP-positive round-shaped cells, and they died within 2 weeks

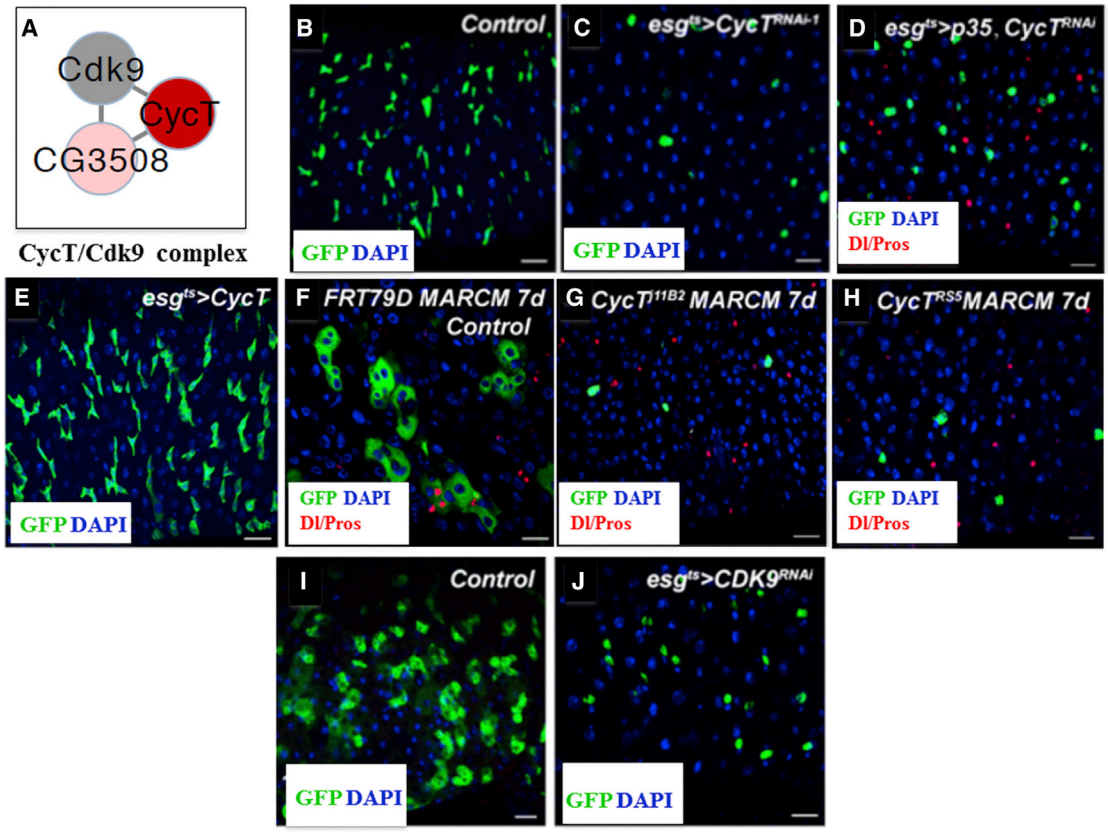

Figure 5. The CycT/Cdk9 Complex Regulates ISC Quiescence/Death

(A) Diagram of the CycT/Cdk9 complex.
(B) *esg*^{ts} wild-type control.
(C) Knockdown of *CycT* resulted in ISC quiescence/death.
(D) Expression of *p35* partially rescued the knockdown phenotype of *CycT*.
(E) Overexpression of *CycT* promoted ISC proliferation.
(F) Control *FRT*^{79D} MARCM clones 7 days ACI.
(G) *FRT*^{79D}-*CycT*^{11B2} MARCM clones 7 days ACI.
(H) *FRT*^{79D}-*CycT*^{RS5} MARCM clones 7 days ACI.
(I) *esg*^{ts} wild-type control.
(J) Knockdown of *Cdk9* resulted in ISC quiescence/death.
The posterior midguts of corresponding flies were dissected, stained with the indicated antibodies, and analyzed by confocal microscopy. The flies were cultured at 29°C for 7 days in (A–E), and 14 days in (I–J). Scale bars represent 10 μm.
See also Figure S2 and Table S1D.

(Figure 5C). Coexpression of the pan-caspase inhibitor p35 could partially slow the death of these GFP-positive cells (Figure 5D). We further generated *CycT* mutant mosaic clones using the MARCM technique (Lee and Luo, 1999) and found that a few single isolated GFP-positive round-shaped ISCs were detected in CycT MARCM clones (compare Figures 5G and 5H with the control in Figure 5F), similar to phenotypes observed in *CycT* RNAi knockdown flies (Figure 5C). Coexpression of p35 in *CycT* MARCM clones could significantly rescue the ISC quiescence/death phenotypes (Figure S2J), but the rescued cells eventually died 14 days after clone induction (ACI) (Figure S2K). Furthermore, overexpression of *CycT* promoted ISC proliferation (Figure 5E). The CycT protein is ubiquitously expressed in posterior midgut (Figure S2G) and specifically expressed in GFP-positive cells in *esg*^{ts} > *CycT* flies (Figure S2H). Cdk9/CycT forms a functional complex in vivo and regulates transcriptional elongation and RNA processing through phosphorylating the carboxyl-terminal domain (CTD) of RNA polymerase II (Pol II) (Ni et al., 2004; Figure 5A). We knocked down *Cdk9* activity using its transgenic RNAi line and found a weaker but similar phenotype compared to that of *CycT* knockdown (compare Figure 5J with Figure 5I).

Genes Whose Knockdowns Resulted in ISC-to-EC Differentiation

Knockdowns of genes required for ISC maintenance or self-renewal would result in the premature differentiation of ISC to EC or EE cells. From our screen, we identified 98 genes whose

RNAi-mediated knockdowns resulted in premature ISC-to-EC differentiation (Figure 2G; Table S1E).

Negative Regulators of the N Pathway

Among the 98 genes, we identified eight negative regulators of the N signal transduction network: *Vps22/lsn*, *Vps36*, *Vps25* (Figures 3B and 3C), *Vps28*, *Vps23/TSG101*, *Hey*, *da*, and *Smr* (Table S1E) (Bray, 2006; Fortini, 2009; Guruharsha et al., 2012). The first five genes function in endosome protein sorting (Figure 3B) and regulate processing of either N or Dl, and the last three are transcriptional factors and control expression of downstream targets of the N signaling. Knockdowns of these genes likely activated the N signaling and promoted ISC-to-EC differentiation. In addition to the known components in the N pathway, we identified five other genes (*CG18398/Tango6*, *CG4722/bib*, *CG14084/Bet1*, *CG4214/Syx5*, and*CG15811/Rop*) (Table S1E) involved in protein processing or exocytosis. These genes may also negatively regulate the N signaling through regulating the processing of N or Dl.

The Mediator Complex

Among the 98 genes, we also identified ten components in the mediator complex: CG4184/MED15, CG5121/MED28, CG1245/MED27, CG18780/MED20, CG6884/MED11, CG31390/MED7, CG1057/MED31, CG12031/MED14, CG13867/MED8, and CG8491/MED12/kto (Figure 3D and E; Table S1E). The mediator complex is a multiple protein complex with 33 identified components in *Drosophila* (Poss et al., 2013). It is involved in nearly all stages of Pol II transcription, including initiation, promoter escape, elongation, pre-mRNA processing, and termination (Conaway and Conaway, 2013). The mediator complex also generally bridges sequence-specific, DNA-binding TFs to the Pol II enzyme, thereby converting biological inputs (communicated by TFs) to physiological responses (via changes in gene expression) (Conaway and Conaway, 2013; Poss et al., 2013). In the posterior midgut, the mediator complex may perform a function similar to that of the aforementioned negative regulators in the N signal transduction pathway, and restrict activation of the N signaling. It will be interesting to determine how the mediator complex regulates N signaling in future studies.

Nucleosome Remodeling and Histone Modification

In addition to the genes described earlier, we identified 74 other genes (Table S1E), whose RNAi-mediated knockdowns resulted in premature ISC-to-EC differentiation. Among them are eight genes involved in nucleosome remodeling and histone modification: *CG10272/gpp/dDot1*, *CG32067/simj*, *CG31865/Ada1-1*, *CG8068/dPIAS*, *CG8103/Mi-2*, *CG4236/Caf1*, *CG7776/E(Pc)*, and *CG4643/Nurf-38*. The data provide a rich resource for investigating ISC-to-EC lineage differentiation in future studies.

Genes Important for ISC-to-EE Cell Differentiation

Extrinsic Slit-Robo2 Signaling from EE Cells to ISCs Regulates the Number of EE Cells through a Negative Feedback Mechanism

Loss-of-function mutations in the N signal transduction pathway resulted in expansion of both ISCs and EE cells (Micchelli and Perrimon, 2006; Ohlstein and Spradling, 2006; Table S1A). Two TFs, Scute (Sc) and Asense (Ase), have been shown, by mRNA profiling, to play a major role in EE cell fate determination and to be upregulated in the midgut that expressed a dominant-negative form of N (N^{DN}) (Bardin et al., 2010). Recent work has demonstrated that EE cells are directly generated from ISCs and that the *AS-C* complex regulates ISCs' commitment to EE cells through Pros (Biteau and Jasper, 2014; Zeng and Hou, 2015). The *AS-C* complex includes four genes: *achaete* [*ac*], *scute* [*sc*], *lethal of scute* [*l(1)sc*], and *asense* [*ase*]). Overexpression of each of the four genes resulted in an increase of EE numbers to different degrees (Table S1F). We also identified a Roundabout receptor (Robo2/leak) in the ISC screen (Table S1F), whose knockdown in ISCs (compare Figure S3B with Figure S3A; Figures S3C and S3D), but not in EBs (compare Figure S3F with Figure S3E; Figures S3G and S3H), resulted in a significant increase in the proportion of Pros-positive EE cells. We further generated GFP-marked ISC clones that are homozygous for the loss-of-function allele lea^2 (Figure S3J), using the MARCM technique. Seven days ACI, we found that the proportion of Pros+ EE cells was significantly increased in the GFP-marked clones of lea^2 (Figures S3J and S3K), as compared with their wild-type counterparts (Figures S3I and S3K), while the ISCs in the GFP-marked clones exhibited normal proliferation and self-renewal (Figure S3L). In addition, we examined posterior midguts of 40-day-old lea^2 heterozygous mutant flies and found that the number of Pros+ EE cells was significantly higher in the lea^2/+ flies (Figure 6B) than in the wild-type flies (Figure 6A).

Robo2 is one of the three receptors (Robo1, Robo2, and Robo3) of a secreted ligand Slit, and the Slit-Robo signal transduction pathway regulates various biological processes (Ypsilanti et al., 2010). We examined the expression of Robo1, Robo2, Robo3, and Slit using their respective antibodies and a LacZ reporter line that is under the *slit* promoter ($Slit^{PZ05248}$). We found that Robo2 was expressed mainly in Esg-positive ISCs and EBs (Figures S4A and S4A′) in wild-type posterior midgut, but not in the Robo2-depleted posterior midgut ($esg^{ts} > lea^{RNAi}$) (Figures S6D and S6D′), suggesting that the RNAi effectively depleted Robo2 protein expression. We could not detect expression of Robo1 and Robo3 in posterior midgut (Figures S6A–S6C′). Furthermore, in our genome-wide RNAi screen, we screened one Robo1 RNAi line ($esg^{ts} > robo1^{RNAi(v42579)}$) and two Robo3 RNAi lines ($esg^{ts} > robo3^{RNAi(v44702)}$ and $esg^{ts} > robo3^{RNAi(JF03331)}$) and did not find any abnormal phenotype (data not shown). Together, these data suggest that only Robo2 functions in the posterior midgut.

It is interesting that the *slit-lacZ* reporter was strongly expressed in Pros-positive EE cells (Figures S4B and S4B′) and weakly expressed ISCs (Figures S5A–S5E); the Slit protein is strongly expressed in EE cells and also weakly expressed in the periphery of Esg-positive ISCs and EBs (Figures S4C and S4C′). The secreting Slit protein may be diffused from EE cells to ISCs and then trapped there by the Robo2 receptor. To further test this hypothesis, we knocked down *lea* in ISCs and EBs by expressing the *lea RNAi*, using esg^{ts}. Reducing the expression of *Robo2/lea* in ISCs and EBs was sufficient to reduce the amount of Slit protein near the periphery of these cells without affecting its expression in EE cells (Figures S4D, S4D′, and S4F). Conversely, we overexpressed *Robo2/lea* in ISCs and EBs by expressing an *UAS-lea* (lea^{EP2582}) using esg^{ts}. As expected, increasing the expression of *Robo2/lea* in ISCs and EBs was sufficient to increase the accumulation of Slit protein

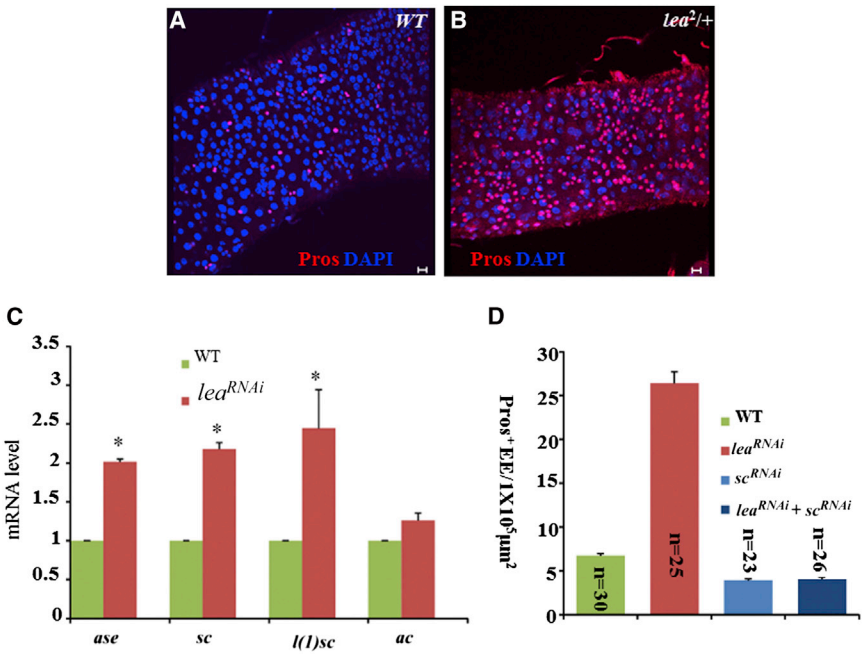

Figure 6. The Slit-Robo2 Signaling Regulates EE Cell Fate Specification Parallel to the AS-C Complex in ISCs

(A and B) The number of Pros+ EE cells is significantly greater in the $lea^{2/+}$ flies (B) than in the wild-type (WT) flies (A). Scale bars represent 10 μm.

(C) mRNA levels of the *AS-C* complex genes in flies of wild-type and ISC^{ts}>> lea^{RNAi}.

(D) Knockdown of both *sc* and *lea* in ISCs (ISC^{ts} > lea^{RNAi} + sc^{RNAi}) suppressed the phenotype of excess EE cells associated with knockdown of *lea* alone.

See also Figures S3–S7 and Table S1F.

at the periphery of these cells without affecting its expression in EE cells (Figures S4E, S4E′, and S4F). These data, taken together, indicate that EE-cell-produced Slit may prevent new EE cell formation by binding Robo2 and activating the Slit-Robo2 signal transduction pathway in ISCs.

To further test this model, we knocked down Slit expression in EE cells using Gal4 (386Y-Gal4), which is specifically expressed in EE cells during larval stages and in EE cells and other cell types in adult posterior midgut (Reiher et al., 2011), and two independent *slit* RNAi lines. In both cases, we observed a small but consistent increase in the proportion of EE cells in the posterior midgut epithelium (Figures S7A and S7B). We also knocked down Slit expression in ISCs (ISC^{ts} > $slit^{RNAi}$) and did not find a significant change of EE cells (Figure S7C). The Slit protein expression could not be detected in the RNAi-knocked-down posterior midgut (Figures S6E–S6H), suggesting that the RNAi effectively depleted Slit protein expression.

In summary, these data suggest that extrinsic Slit-Robo2 signaling from EE cells to ISCs regulates the proportion of EE cells through a negative feedback mechanism to keep the right balance of differentiated cells in the posterior midgut epithelium.

Slit-Robo2 Signaling Regulates EE Cell Fate Specification Either Upstream or in Parallel to AS-C Complex in ISCs

To determine which transcription factor mediates Slit-Robo2 signaling in ISCs to regulate EE cell generation, we first overexpressed *pros* in ISCs and EBs (esg^{ts} > *pros*) because Pros is an EE cell marker and closely associated with EE cell fate specification (described earlier). Overexpression of Pros in ISCs and EBs did not affect the proportion of EE cells but rather promoted ISC/EB-to-EC differentiation in the posterior midgut epithelium (Figure S5F), indicating that knocking down the Slit-Robo2 signal does not increase the number of EE cells through inducing *pros* expression.

Sc and Ase play a major role in EE cell fate determination (Bardin et al., 2010; Zeng et al., 2013; Zeng and Hou, 2015). To examine the relationship of Robo2/lea to Sc and Ase, we first compared mRNA levels of the *AS-C* genes in the midguts of wild-type and ISC^{ts} > lea^{RNAi} flies, using qPCR. Among the four *AS-C* genes, the mRNA levels of *ase*, *sc*, and *l(1)sc* were significantly upregulated in ISC^{ts} > lea^{RNAi} midguts, while the mRNA level of *ac* did not significantly change in comparison to that in wild-type midguts (Figure 6C). We further expressed sc^{RNAi} in the ISC^{ts} > lea^{RNAi} midgut (ISC^{ts} > lea^{RNAi} +sc^{RNAi}; Figure 6D) and found that the expression of sc^{RNAi} in the lea^{RNAi} midgut suppressed the excess EE cell phenotype of lea^{RNAi} (Figure 6D). Together, our data so far suggest that the Slit-Robo2 signaling regulates EE cell fate specification either upstream or in parallel to the *AS-C* complex in ISCs.

In addition to the genes described earlier, we identified 16 other genes whose RNAi-mediated knockdowns affect differentiation from ISCs to EE cells (Table S1F). The data provide a rich resource for investigating ISC-to-EE lineage differentiation in future studies.

Comparison of Genes that Regulate ISCs, Female GSCs, and Neural Stem Cells

We compared our results with previous screens in Nbs (Neumüller et al., 2011) and female GSCs (Yan et al., 2014) to identify common or unique factors that regulate self-renewal and differentiation of different stem cell systems (Figure 7A). Neural stem cell (NSC) self-renewal and differentiation are controlled through intrinsic asymmetric division, while the fates of female GSCs are regulated through a local niche-dependent mechanism. The adult *Drosophila* ISCs are regulated by signals from multiple directions, including underlying visceral muscle cells (reviewed in Jiang and Edgar, 2011; O'Brien et al., 2011), differentiated ECs during tissue damage and bacterial infection (Jiang and Edgar, 2011), and trachea-derived Dpp (Li et al., 2013). Because all three stem cell types are actively dividing, self-renewing, and generating lineage-specific differentiated cells, we expected that some of the basic cellular processes are commonly

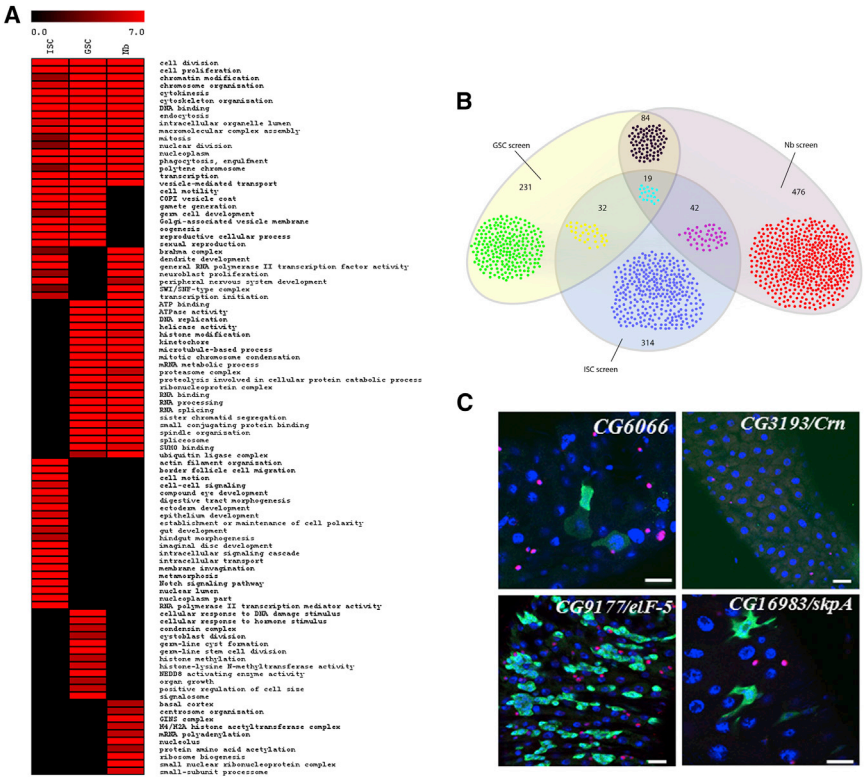

Figure 7. Comparison of ISC, Nb, and Female GSC RNAi Screens

(A) Heatmap display overrepresentation of selected GO terms associated with genes identified in the ISC, Nb, and female GSC screens.

(B) Number of genes identified in the ISC, Nb, and female GSC screens. In all, 19 genes were found in all three screens. Another 32 genes were identified in both ISC and female GSC screens, and the other 42 genes were identified in both ISC and Nb screens.

(C) Phenotypes of common genes identified in ISC, female GSC, and NSC screens. Scale bars represent 5 μm.

See also Tables S1 and S4.

required and that the stem-cell-specific regulatory signals are different.

Among the 405 genes identified in the ISC screen, 19 were identified in all three screens, another 31 genes were identified in both ISC and female GSC screens, and the other 43 genes were identified in both ISC and NSC screens (Figure 7B; Table S4). Most of the shared genes are regulators of basic cellular processes.

Knockdown of several components (*osa*, *brm*, *Snar1*, and *dalao*) of the Brahma (BRM) chromatin-remodeling complex resulted in an expansion of stem-cell-like cells in both ISCs and type II Nb lineages (Neumüller et al., 2011; Zeng et al., 2013; Table S1) while knockdown of these genes in female GSC lineage was without detectable phenotypes (Yan et al., 2014). On the other hand, knockdown of several components of the COPI complex resulted in ISC-specific cell death (Figure 7E; Table S1D) and defects in female GSC lineage (Yan et al., 2014), but none of these genes were identified in the Nbs screen (Neumüller et al., 2011). Most of the genes involved in the signal transduction pathways identified in our screen are ISC specific. As mentioned before, the N signal transduction pathway plays a major role in regulating ISC self-renewal and differentiation. We identified 19 positive and 8 negative regulators of the N pathway in our ISC screen (Tables S1 and S4), but only two positive regulators (*Dl* and *aux*) were identified in the female GSC screen and one negative regulator (*da*) was identified in the Nbs screen (Neumüller et al., 2011; Yan et al., 2014; Table S4). Most of the genes required for ISC proliferation are ISC specific, including components in the EGFR, JAK-Stat, Dpp, JNK, and Hippo signal transduction pathways (Tables S1 and S4).

In summary, factors related to basic stem cell cellular processes are commonly required in all stem cells, and stem-cell-specific, niche-related signals are only required in the unique stem cell type.

DISCUSSION

Drosophila midgut stem cells provide an excellent genetic system for studying tissue homeostasis, regeneration, hyperplasia, stress, and aging (Amcheslavsky et al., 2009; Buchon et al., 2009a, 2009b; Biteau et al., 2008; Buszczak et al., 2009; Cronin et al., 2009; Hochmuth et al., 2011; Jiang et al., 2009, 2011; Jin et al., 2013; Wang et al., 2014; Zeng et al., 2013). In the past few years, using homozygous mutant animals or mosaic analyses, several genes have been identified to be required in ISC self-renewal and differentiation. However, a systematic molecular understanding of self-renewal and lineage-specific differentiation of adult ISCs has not been performed. Here, we screened 44.8% of the fly genome and identified 405 genes that regulate various fates of adult *Drosophila* ISCs. Since we screened the RNAi lines giving an adult lethal phenotype, we might have missed some adult gut-specific genes in this screen. Nevertheless, the genes identified here, we further obtained precise quantification of phenotypic data and identified regulatory networks through a computer network analysis. From our phenotype and network analysis, we reached a number of important conclusions. First, ISC self-renewal, EE cell fate determination, and EB differentiation are regulated by distinct networks or pathways (Table S1A). The JAK-Stat pathway regulates EB differentiation; some components in the N signal transduction network control both ISC self-renewal and EE cell fate determination, and knockdowns of these components resulted in expansion of both ISCs and EE cells. The other components in the N signal transduction network control only ISC self-renewal, and knockdowns of those components resulted only in ISC expansion. The way that the Brm/Osa complex regulates ISC self-renewal and EE cell fate determination is different from that of the N signaling; knockdowns of the components in the Brm/Osa complex resulted in ISC expansion and EE cell reduction. Second, ISC proliferation

is uniquely regulated. Very few genes whose knockdowns resulted in ISC overproliferation in the ISC screen were also isolated in the screens of Nbs and female GSCs (Neumüller et al., 2011; Yan et al., 2014; Table S4), suggesting that these genes and signal transduction pathways regulate ISC proliferation only. Third, knockdowns of several regulators of mitotic cell cycle and mitotic cytokinesis resulted in large nuclei (polyploidy) in ISCs and EE cells, suggesting that the cell-cycle regulators uniquely maintain diploid cells. Fourth, we found that the COPI and CycT/Cdk9 complexes specifically regulate ISC survival. Quiescent CSCs are often resistant to traditional cancer therapies that primarily target dividing and actively metabolizing cells (Trumpp and Wiestler, 2008). Studying stem cell death using the data generated from this screen may lead to the design of new therapies to selectively eliminate stem cells in cancer. Fifth, we identified a large mediator complex that regulates ISC-to-EC differentiation. Sixth, we found that the Slit/Robo2-negative feedback pathway, the N inhibitory pathway, and the Brm/Osa complex together regulate EE cell fate specification in ISCs, either upstream or in parallel to AS-C/Pros. Seventh, by comparing genes identified in screens of ISCs, Nbs, and female GSCs, we found that factors related to the cellular processes of basic stem cells are commonly required in all stem cells, and stem-cell-specific, niche-related signals are required only in the unique stem cell type. The information obtained from this study will help to further dissect the regulatory networks in stem cell biology.

EXPERIMENTAL PROCEDURES

Fly Stocks

The following fly strains were used: *esg-Gal4* line (from Shigeo Hayashi); *Su(H)GBE-Gal4* (Zeng et al., 2010), *Su(H)GBE-tub-Gal80*, and *ISC*^{ts} [*esg-Gal4, UAS-GFP; tub-Gal80*^{ts}, *Su(H)GBE-tub-Gal80*] (Zeng and Hou, 2015); and *UAS-CycT*, which was generated in our laboratory. The Bloomington *Drosophila* Stock Center (BDSC) supplied the following strains: *tub-Gal80*^{ts}, *lea*^{2}, *lea*^{EP2582}, *UAS-p35*, *N*$^{264-39}$, *UAS-lea*^{RNAi} (BL9286), *slit*^{PZ05248}, *UAS-slit*$^{RNAi-1}$ (BL31468), *UAS-robo3*$^{RNAi-1}$ (BL29398), *UAS-CycT*$^{RNAi-1}$ (BL31762), *UAS-CycT*$^{RNAi-2}$ (BL32976), *UAS-Cdk9*^{RNAi} (BL34982), *CycT*^{11B2} (BL12101); as well as fly lines used for MARCM clones, including *FRT*^{2A}*-piM*, *FRT*^{40A}*-piM*, *SM6,hs-flp*, *MKRS,hs-flp*, *FRT*^{2A} *tub-Gal80*, *FRT*^{40A} *tub-Gal80*, and *FRT*^{19A} *tub-Gal80*. The following transgenic RNAi lines were obtained from VDRC: *UAS-slit*$^{RNAi-2}$ (v108853), *UAS-robo1*^{RNAi} (v42579), and *UAS-robo3*$^{RNAi-2}$ (v44702). *CycT*^{RS5} (Kyoto125610) was from the Kyoto *Drosophila* Stock Center.

Flies were raised on standard fly food at 25°C and 65% humidity, unless otherwise indicated.

RNAi Stocks Used in the Screen

UAS-RNAi lines were generated by the VDRC and the Transgenic RNAi Project (TRiP) and are available at the VDRC and the BDSC. The sequences used for VDRC knockdown strains are available for each line at https://stockcenter.vdrc.at), and those for Bloomington knockdown strains are available for each line at http://flystocks.bio.indiana.edu.

MARCM Clonal Analysis

To induce MARCM clones of *FRT*^{2A}*-piM* (as a wild-type control), *FRT*^{2A}*-CycT*^{11B2}, *FRT*^{2A}*-CycT*^{RS5}, *FRT*^{40A}*-piM* (as a wild-type control), *FRT*^{40A}*-lea*^{2}, *FRT*^{19A}*-sn*^{3} *w*^{1118} (as a wild-type control), and *FRT*^{19A}*-N*$^{264-39}$, we generated the following flies: *act>y*$^{+}$ > *Gal4, UAS-GFP/SM6, hs-flp; FRT*^{2A} *tub-Gal80/ FRT*^{2A} *mutant* or *FRT*^{40A} *tub-Gal80/FRT*^{40A} *mutant;* and *MKRS, hs-flp/ act* > *CD2* > *Gal4, UAS-GFP* or *hs-flp, tub-Gal80, FRT*^{19A}*/ FRT*^{19A} *mutant*; and *act>y*$^{+}$ > *Gal4, UAS-GFP*/+. Three- or 4-day-old adult female flies were heat shocked at 37°C for 45 min twice, at an interval of 8–12 hr. The flies were transferred to fresh food daily after the final heat shock, and their posterior midguts were processed for staining at the indicated times.

RNAi-Mediated Gene Depletion

Male *UAS-RNAi* transgene flies were crossed with female virgins of *esg-Gal4, UAS-GFP; tub-Gal80*^{ts}, *esg-Gal4,UAS-GFP; Su(H)GBE-Gal80, tub-Gal80*^{ts} (for ISC-specific expression), *Su(H)GBE-Gal4,UAS-GFP; tub-Gal80*^{ts} (for EB-specific expression), or *UAS-mCD8.GFP*; *esg-Gal4,wg-Gal4; tub-Gal80*^{ts} (for expression in both posterior midgut and hindgut ISCs). The flies were cultured at 18°C. Three- to 5-day-old adult flies with the appropriate genotype were transferred to new vials at 29°C for 7 days or 14 days before dissection.

Histology and Image Capture

The fly intestines were dissected in PBS and fixed in PBS containing 4% formaldehyde for 20 min. After three 5-min rinses with PBT (PBS + 0.1% Triton X-100), the samples were blocked with PBT containing 5% normal goat serum and kept overnight at 4°C. Then, the samples were incubated with primary antibody at room temperature for 2 hr and incubated with the fluorescence-conjugated secondary antibody for 2 hr at room temperature. Samples were mounted in the Vectashield mounting medium with DAPI (Vector Laboratories). We used the following antibodies: mouse anti-β-Gal (1:200; Clontech); mouse anti-Dl (1:50; Developmental Studies Hybridoma Bank [DSHB]); mouse anti-Pros (1:50; DSHB); nc82 (1:20; DSHB); anti-Slit (1:20; DSHB); guinea pig anti-Pros (1:3,000, a gift from Tiffany Cook); rabbit anti-Robo2 (1:100, a gift from Barry Dickson); mouse anti-Robo1 (1:50; DSHB); mouse anti-Robo3 cytoplasmic (15H2) (1:50; DSHB); mouse anti-Robo3 extracellular (14C9) (1:50; DSHB); rabbit anti-CycT (1:1,000; generated in X.L.'s laboratory), and chicken anti-GFP (1:3,000; Abcam). Secondary antibodies used were goat anti-mouse, anti-chicken, anti-guinea pig, and anti-rabbit immunoglobulin G conjugated to Alexa Fluor 488 or Alexa Fluor 568 (1:400; Molecular Probes). Images were captured with the Zeiss LSM 510 confocal system and processed with the LSM Image Browser and Adobe Photoshop.

Quantification and Statistical Analysis

To quantify the percentage of Pros^{+} EE cells (except for Figures S7A–S7H, in which the Pros^{+} EE cells and total cells were counted in a 1 × 10^{5} μm^{2} area of a z stack of multiple confocal planes), the Pros^{+} EE cells and total cells were counted in a 1 × 10^{5} μm^{2} area of a single confocal plane. To quantify the strength of fluorescence of Slit staining, all the images were taken with the same confocal settings, and the fluorescence intensity was measured using an LSM5 Image Browser (Zeiss). All the data were analyzed using Student's t test, and sample sizes (n) are shown in all figures with error bars.

SUPPLEMENTAL INFORMATION

Supplemental Information includes Supplemental Experimental Procedures, seven figures, and five tables and can be found with this article online at http://dx.doi.org/10.1016/j.celrep.2015.01.051.

AUTHOR CONTRIBUTIONS

X.Z., S.X.H., and X.L. conceived and designed the experiments. X.Z., S.R.S., L.H., H.L., Y.L., W.L., and S.X.H. performed the experiments. R.A.N., D.Y., S.R.S., and Y.H. performed the bioinformatics. X.Z., S.R.S., S.X.H., and X.L. analyzed the data. S.X.H., S.R.S., and X.Z. wrote and revised the manuscript, L.H. and S.R.S. made equal contributions in performing experiments, and all authors approved the final version of the manuscript.

ACKNOWLEDGMENTS

We thank Shigeo Hayashi, Tiffany Cook, VDRC, the Bloomington Stock Centers, and TRiP at Harvard Medical School for fly stocks; Barry Dickson, Tiffany Cook, and DSHB for antibodies; and S. Lockett for help with the confocal microscope. Work in the laboratory of S.X.H. was supported by the Intramural Research Program of the National Cancer Institute; work in the laboratory of

X.L. was supported by grants from the Nature Sciences Foundation of China (31030049, 81361120382, and 31271582) and the Strategic Priority Research Program of the Chinese Academy of Sciences Grant (XDA01010101).

Received: August 3, 2014
Revised: November 6, 2014
Accepted: January 16, 2015
Published: February 19, 2015

REFERENCES

Amcheslavsky, A., Jiang, J., and Ip, Y.T. (2009). Tissue damage-induced intestinal stem cell division in *Drosophila*. Cell Stem Cell *4*, 49–61.

Amcheslavsky, A., Ito, N., Jiang, J., and Ip, Y.T. (2011). Tuberous sclerosis complex and Myc coordinate the growth and division of *Drosophila* intestinal stem cells. J. Cell Biol. *193*, 695–710.

Bardin, A.J., Perdigoto, C.N., Southall, T.D., Brand, A.H., and Schweisguth, F. (2010). Transcriptional control of stem cell maintenance in the *Drosophila* intestine. Development *137*, 705–714.

Baumbach, J., Hummel, P., Bickmeyer, I., Kowalczyk, K.M., Frank, M., Knorr, K., Hildebrandt, A., Riedel, D., Jäckle, H., and Kühnlein, R.P. (2014). A Drosophila in vivo screen identifies store-operated calcium entry as a key regulator of adiposity. Cell Metab. *19*, 331–343.

Beebe, K., Lee, W.C., and Micchelli, C.A. (2010). JAK/STAT signaling coordinates stem cell proliferation and multilineage differentiation in the *Drosophila* intestinal stem cell lineage. Dev. Biol. *338*, 28–37.

Beller, M., Sztalryd, C., Southall, N., Bell, M., Jäckle, H., Auld, D.S., and Oliver, B. (2008). COPI complex is a regulator of lipid homeostasis. PLoS Biol. *6*, e292.

Berns, N., Woichansky, I., Friedrichsen, S., Kraft, N., and Riechmann, V. (2014). A genome-scale in vivo RNAi analysis of epithelial development in Drosophila identifies new proliferation domains outside of the stem cell niche. J. Cell Sci. *127*, 2736–2748.

Biteau, B., and Jasper, H. (2011). EGF signaling regulates the proliferation of intestinal stem cells in *Drosophila*. Development *138*, 1045–1055.

Biteau, B., and Jasper, H. (2014). Slit/Robo signaling regulates cell fate decisions in the intestinal stem cell lineage of *Drosophila*. Cell Rep. *7*, 1867–1875.

Biteau, B., Hochmuth, C.E., and Jasper, H. (2008). JNK activity in somatic stem cells causes loss of tissue homeostasis in the aging *Drosophila* gut. Cell Stem Cell *3*, 442–455.

Bray, S.J. (2006). Notch signalling: a simple pathway becomes complex. Nat. Rev. Mol. Cell Biol. *7*, 678–689.

Buchon, N., Broderick, N.A., Poidevin, M., Pradervand, S., and Lemaitre, B. (2009a). *Drosophila* intestinal response to bacterial infection: activation of host defense and stem cell proliferation. Cell Host Microbe *5*, 200–211.

Buchon, N., Broderick, N.A., Chakrabarti, S., and Lemaitre, B. (2009b). Invasive and indigenous microbiota impact intestinal stem cell activity through multiple pathways in *Drosophila*. Genes Dev. *23*, 2333–2344.

Buszczak, M., Paterno, S., and Spradling, A.C. (2009). *Drosophila* stem cells share a common requirement for the histone H2B ubiquitin protease scrawny. Science *323*, 248–251.

Clevers, H. (2013). The intestinal crypt, a prototype stem cell compartment. Cell *154*, 274–284.

Conaway, R.C., and Conaway, J.W. (2013). The Mediator complex and transcription elongation. Biochim. Biophys. Acta *1829*, 69–75.

Cronin, S.J., Nehme, N.T., Limmer, S., Liegeois, S., Pospisilik, J.A., Schramek, D., Leibbrandt, A., Simoes Rde., M., Gruber, S., Puc, U., et al. (2009). Genome-wide RNAi screen identifies genes involved in intestinal pathogenic bacterial infection. Science *325*, 340–343.

Dietzl, G., Chen, D., Schnorrer, F., Su, K.C., Barinova, Y., Fellner, M., Gasser, B., Kinsey, K., Oppel, S., Scheiblauer, S., et al. (2007). A genome-wide transgenic RNAi library for conditional gene inactivation in *Drosophila*. Nature *448*, 151–156.

Fortini, M.E. (2009). Notch signaling: the core pathway and its posttranslational regulation. Dev. Cell *16*, 633–647.

Guo, Z., Driver, I., and Ohlstein, B. (2013). Injury-induced BMP signaling negatively regulates *Drosophila* midgut homeostasis. J. Cell Biol. *201*, 945–961.

Guruharsha, K.G., Kankel, M.W., and Artavanis-Tsakonas, S. (2012). The Notch signalling system: recent insights into the complexity of a conserved pathway. Nat. Rev. Genet. *13*, 654–666.

Hakim, R.S., Baldwin, K., and Smagghe, G. (2010). Regulation of midgut growth, development, and metamorphosis. Annu. Rev. Entomol. *55*, 593–608.

Hochmuth, C.E., Biteau, B., Bohmann, D., and Jasper, H. (2011). Redox regulation by Keap1 and Nrf2 controls intestinal stem cell proliferation in *Drosophila*. Cell Stem Cell *8*, 188–199.

Ito, K., and Suda, T. (2014). Metabolic requirements for the maintenance of self-renewing stem cells. Nat. Rev. Mol. Cell Biol. *15*, 243–256.

Jiang, H., and Edgar, B.A. (2011). Intestinal stem cells in the adult *Drosophila* midgut. Exp. Cell Res. *317*, 2780–2788.

Jiang, H., Patel, P.H., Kohlmaier, A., Grenley, M.O., McEwen, D.G., and Edgar, B.A. (2009). Cytokine/Jak/Stat signaling mediates regeneration and homeostasis in the *Drosophila* midgut. Cell *137*, 1343–1355.

Jiang, H., Grenley, M.O., Bravo, M.J., Blumhagen, R.Z., and Edgar, B.A. (2011). EGFR/Ras/MAPK signaling mediates adult midgut epithelial homeostasis and regeneration in *Drosophila*. Cell Stem Cell *8*, 84–95.

Jin, Y., Xu, J., Yin, M.X., Lu, Y., Hu, L., Li, P., Zhang, P., Yuan, Z., Ho, M.S., Ji, H., et al. (2013). Brahma is essential for *Drosophila* intestinal stem cell proliferation and regulated by Hippo signaling. eLife *2*, e00999.

Karpowicz, P., Perez, J., and Perrimon, N. (2010). The Hippo tumor suppressor pathway regulates intestinal stem cell regeneration. Development *137*, 4135–4145.

Lee, T., and Luo, L. (1999). Mosaic analysis with a repressible cell marker for studies of gene function in neuronal morphogenesis. Neuron *22*, 451–461.

Lee, M.C., Miller, E.A., Goldberg, J., Orci, L., and Schekman, R. (2004). Bi-directional protein transport between the ER and Golgi. Annu. Rev. Cell Dev. Biol. *20*, 87–123.

Li, Z., Zhang, Y., Han, L., Shi, L., and Lin, X. (2013). Trachea-derived dpp controls adult midgut homeostasis in *Drosophila*. Dev. Cell *24*, 133–143.

Li, Q., Li, S., Mana-Capelli, S., Roth Flach, R.J., Danai, L.V., Amcheslavsky, A., Nie, Y., Kaneko, S., Yao, X., Chen, X., et al. (2014). The conserved misshapen-warts-Yorkie pathway acts in enteroblasts to regulate intestinal stem cells in Drosophila. Dev. Cell *31*, 291–304.

Ma, Y., Chen, Z., Jin, Y., and Liu, W. (2013). Identification of a histone acetyltransferase as a novel regulator of *Drosophila* intestinal stem cells. FEBS Lett. *587*, 1489–1495.

McGuire, S.E., Le, P.T., Osborn, A.J., Matsumoto, K., and Davis, R.L. (2003). Spatiotemporal rescue of memory dysfunction in *Drosophila*. Science *302*, 1765–1768.

Micchelli, C.A., and Perrimon, N. (2006). Evidence that stem cells reside in the adult *Drosophila* midgut epithelium. Nature *439*, 475–479.

Min, K.T., and Benzer, S. (1999). Preventing neurodegeneration in the *Drosophila* mutant bubblegum. Science *284*, 1985–1988.

Morris, R.J., Liu, Y., Marles, L., Yang, Z., Trempus, C., Li, S., Lin, J.S., Sawicki, J.A., and Cotsarelis, G. (2004). Capturing and profiling adult hair follicle stem cells. Nat. Biotechnol. *22*, 411–417.

Mummery-Widmer, J.L., Yamazaki, M., Stoeger, T., Novatchkova, M., Bhalerao, S., Chen, D., Dietzl, G., Dickson, B.J., and Knoblich, J.A. (2009). Genome-wide analysis of Notch signalling in *Drosophila* by transgenic RNAi. Nature *458*, 987–992.

Muñoz, J., Stange, D.E., Schepers, A.G., van de Wetering, M., Koo, B.K., Itzkovitz, S., Volckmann, R., Kung, K.S., Koster, J., Radulescu, S., et al. (2012). The Lgr5 intestinal stem cell signature: robust expression of proposed quiescent '+4' cell markers. EMBO J. *31*, 3079–3091.

Neely, G.G., Kuba, K., Cammarato, A., Isobe, K., Amann, S., Zhang, L., Murata, M., Elmén, L., Gupta, V., Arora, S., et al. (2010). A global in vivo Drosophila

RNAi screen identifies NOT3 as a conserved regulator of heart function. Cell *141*, 142–153.

Neumüller, R.A., Richter, C., Fischer, A., Novatchkova, M., Neumüller, K.G., and Knoblich, J.A. (2011). Genome-wide analysis of self-renewal in *Drosophila* neural stem cells by transgenic RNAi. Cell Stem Cell *8*, 580–593.

Ni, Z., Schwartz, B.E., Werner, J., Suarez, J.R., and Lis, J.T. (2004). Coordination of transcription, RNA processing, and surveillance by P-TEFb kinase on heat shock genes. Mol. Cell *13*, 55–65.

Ni, J.Q., Zhou, R., Czech, B., Liu, L.P., Holderbaum, L., Yang-Zhou, D., Shim, H.S., Tao, R., Handler, D., Karpowicz, P., et al. (2011). A genome-scale shRNA resource for transgenic RNAi in *Drosophila*. Nat. Methods *8*, 405–407.

O'Brien, L.E., Soliman, S.S., Li, X., and Bilder, D. (2011). Altered modes of stem cell division drive adaptive intestinal growth. Cell *147*, 603–614.

Ohlstein, B., and Spradling, A. (2006). The adult *Drosophila* posterior midgut is maintained by pluripotent stem cells. Nature *439*, 470–474.

Ohlstein, B., and Spradling, A. (2007). Multipotent *Drosophila* intestinal stem cells specify daughter cell fates by differential notch signaling. Science *315*, 988–992.

Palanker, L., Tennessen, J.M., Lam, G., and Thummel, C.S. (2009). *Drosophila* HNF4 regulates lipid mobilization and beta-oxidation. Cell Metab. *9*, 228–239.

Perdigoto, C.N., Schweisguth, F., and Bardin, A.J. (2011). Distinct levels of Notch activity for commitment and terminal differentiation of stem cells in the adult fly intestine. Development *138*, 4585–4595.

Poss, Z.C., Ebmeier, C.C., and Taatjes, D.J. (2013). The Mediator complex and transcription regulation. Crit. Rev. Biochem. Mol. Biol. *48*, 575–608.

Reiher, W., Shirras, C., Kahnt, J., Baumeister, S., Isaac, R.E., and Wegener, C. (2011). Peptidomics and peptide hormone processing in the *Drosophila* midgut. J. Proteome Res. *10*, 1881–1892.

Ren, F., Wang, B., Yue, T., Yun, E.Y., Ip, Y.T., and Jiang, J. (2010). Hippo signaling regulates *Drosophila* intestine stem cell proliferation through multiple pathways. Proc. Natl. Acad. Sci. USA *107*, 21064–21069.

Schnorrer, F., Schönbauer, C., Langer, C.C., Dietzl, G., Novatchkova, M., Schernhuber, K., Fellner, M., Azaryan, A., Radolf, M., Stark, A., et al. (2010). Systematic genetic analysis of muscle morphogenesis and function in Drosophila. Nature *464*, 287–291.

Soni, K.G., Mardones, G.A., Sougrat, R., Smirnova, E., Jackson, C.L., and Bonifacino, J.S. (2009). Coatomer-dependent protein delivery to lipid droplets. J. Cell Sci. *122*, 1834–1841.

Staley, B.K., and Irvine, K.D. (2010). Warts and Yorkie mediate intestinal regeneration by influencing stem cell proliferation. Curr. Biol. *20*, 1580–1587.

Takahashi, K., and Yamanaka, S. (2006). Induction of pluripotent stem cells from mouse embryonic and adult fibroblast cultures by defined factors. Cell *126*, 663–676.

Trumpp, A., and Wiestler, O.D. (2008). Mechanisms of disease: cancer stem cells—targeting the evil twin. Nat. Clin. Pract. Oncol. *5*, 337–347.

Tumbar, T., Guasch, G., Greco, V., Blanpain, C., Lowry, W.E., Rendl, M., and Fuchs, E. (2004). Defining the epithelial stem cell niche in skin. Science *303*, 359–363.

Vinayagam, A., Hu, Y., Kulkarni, M., Roesel, C., Sopko, R., Mohr, S.E., and Perrimon, N. (2013). Protein complex-based analysis framework for high-throughput data sets. Sci. Signal. *6*, rs5.

Wang, C., Chang, K.C., Somers, G., Virshup, D., Ang, B.T., Tang, C., Yu, F., and Wang, H. (2009). Protein phosphatase 2A regulates self-renewal of *Drosophila* neural stem cells. Development *136*, 2287–2296.

Wang, L., Karpac, J., and Jasper, H. (2014). Promoting longevity by maintaining metabolic and proliferative homeostasis. J. Exp. Biol. *217*, 109–118.

Ward, P.S., and Thompson, C.B. (2012). Metabolic reprogramming: a cancer hallmark even warburg did not anticipate. Cancer Cell *21*, 297–308.

Wilson, R.J., Goodman, J.L., and Strelets, V.B.; FlyBase Consortium (2008). FlyBase: integration and improvements to query tools. Nucleic Acids Res. *36*, D588–D593.

Xu, N., Wang, S.Q., Tan, D., Gao, Y., Lin, G., and Xi, R. (2011). EGFR, Wingless and JAK/STAT signaling cooperatively maintain *Drosophila* intestinal stem cells. Dev. Biol. *354*, 31–43.

Yan, D., Neumüller, R.A., Buckner, M., Ayers, K., Li, H., Hu, Y., Yang-Zhou, D., Pan, L., Wang, X., Kelley, C., et al. (2014). A regulatory network of *Drosophila* germline stem cell self-renewal. Dev. Cell *28*, 459–473.

Ypsilanti, A.R., Zagar, Y., and Chédotal, A. (2010). Moving away from the midline: new developments for Slit and Robo. Development *137*, 1939–1952.

Zeng, X., Chauhan, C., and Hou, S.X. (2010). Characterization of midgut stem cell- and enteroblast-specific Gal4 lines in *drosophila*. Genesis *48*, 607–611.

Zeng, X., Lin, X., and Hou, S.X. (2013). The Osa-containing SWI/SNF chromatin-remodeling complex regulates stem cell commitment in the adult *Drosophila* intestine. Development *140*, 3532–3540.

Zhang, Y., Chen, D., and Wang, Z. (2009). Analyses of mental dysfunction-related ACSl4 in *Drosophila* reveal its requirement for Dpp/BMP production and visual wiring in the brain. Hum. Mol. Genet. *18*, 3894–3905.

Zhang, J., Nuebel, E., Daley, G.Q., Koehler, C.M., and Teitell, M.A. (2012). Metabolic regulation in pluripotent stem cells during reprogramming and self-renewal. Cell Stem Cell *11*, 589–595.

Zeng, X., and Hou, S. (2015). Enteroendocrine cells are generated from stem cells through a distinct progenitor in the adult Drosophila posterior midgut. Development *142*, 644–653.

Cell Reports

Supplemental Information

Genome-wide RNAi Screen Identifies Networks Involved in Intestinal Stem Cell Regulation in *Drosophila*

Xiankun Zeng, Lili Han, Shree Ram Singh, Hanhan Liu, Ralph A. Neumüller, Dong Yan, Yanhui Hu, Ying Liu, Wei Liu, Xinhua Lin, and Steven X. Hou

SUPPLEMENTAL DATA

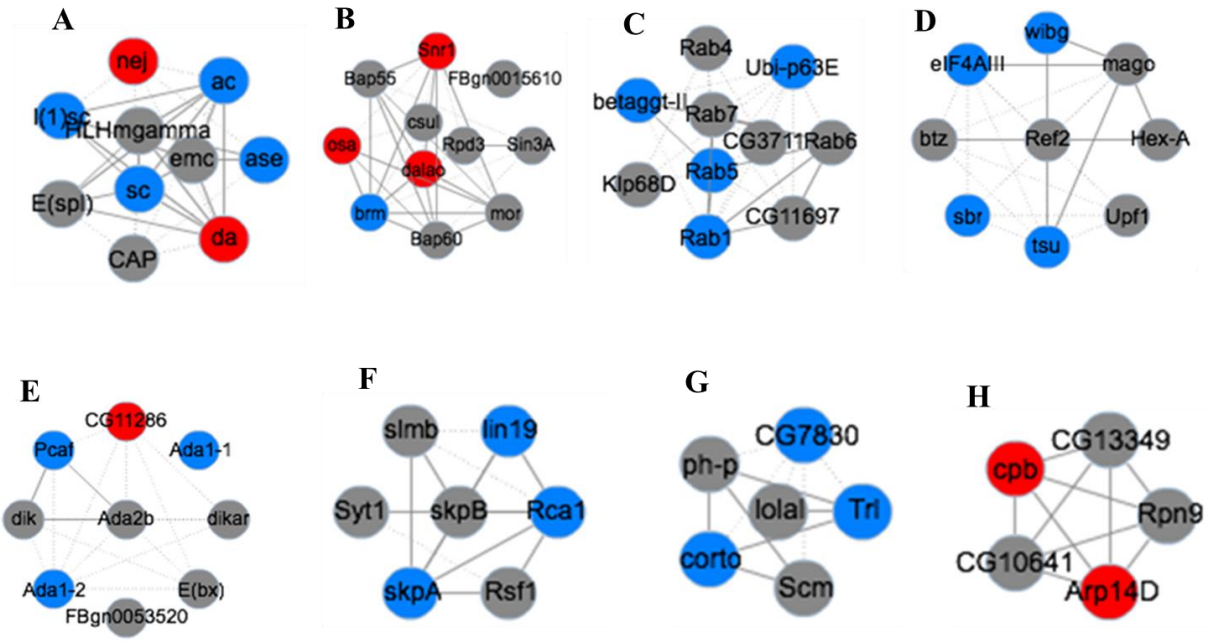

Figure S1, Related to Figure 3. Representive Protein Complexes Identified Using COMPLEAT.
(A) Transcription regulator complex. (B) Diagram of the Brm/Osa complex. (C) Endocytosis complex. (D) Pole plasm oskar mRNA localization complex. (E) Ada2p/Gcn5p/Ada3 transcription activator complex. (F) Uniquitin-dependent protein catabolic process complex. (G) Chromatin silencing complex. (H) Regulation of actin polymerization or depolymerization. Red and blue are genes identified in the screen, grey are genes that are not identified in the screen but were identified by querying publicly available databases. The full list of protein complexes are shown in Table S3.

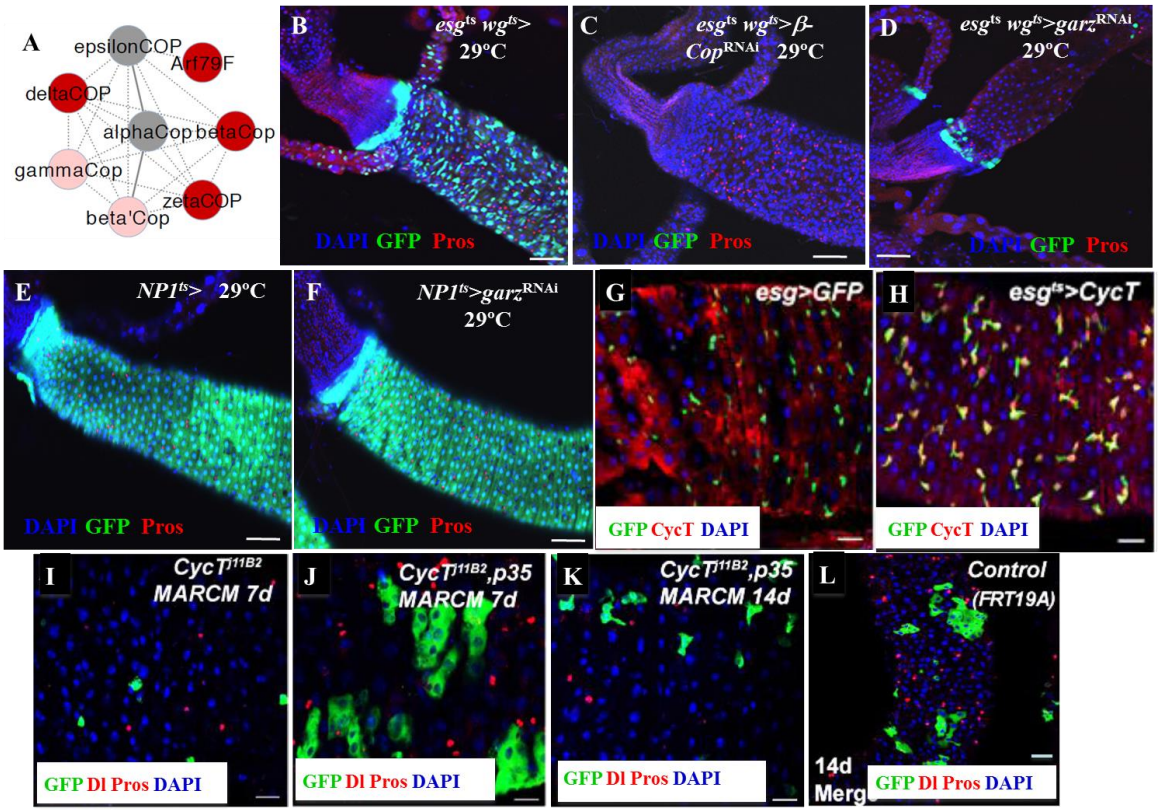

Figure S2. (A-F) Related to Figure 2. Knockdowns of the COPI/Arf79F Complex Resulted in ISC Specific Cell Death. (A) Diagram of the COPI complex. (B-D) Knockdowns of the COPI complex in the posterior midgut intestinal stem cells (ISCs) and hindgut intestinal stem cells (HISCs) using the *esg*^{ts} *wg*^{ts} double Gal4 (*UAS-mCD8.GFP*; *esg-Gal4 wg-Gal4*; *tub-Gal80*^{ts}) resulted in stem cell death. (B) *esg*^{ts} *wg*^{ts}> control, (C) *esg*^{ts} *wg*^{ts}>*β-Cop*^{RNAi}, (D) *esg*^{ts} *wg*^{ts}>*garz*^{RNAi}, (E) *NP1*^{ts}> (*UAS-mCD8.GFP; NP1-Gal4; tub-Gal80*^{ts}) control, (F) *NP1*^{ts}>*garz*^{RNAi}. After cultured the flies at 29°C for 7 days, the posterior midguts of corresponding flies were dissected, stained with antibodies of GFP+Dl+Pros+DAPI, and analyzed by confocal microscopy. Scale bars, 10 μm.

(G-L) Related to Figure 5. The CycT/Cdk9 Complex Regulates ISC Quiescent/Death. (G) CycT protein expression in *esg>GFP* control flies. (H) CycT protein expression in *esg*^{ts}*>CycT* flies. (I) *FRT*^{79D}*-CycT*^{j11B2} MARCM clones 7 days after clonal induction. (J) Expression of *p35* partially rescued the phenotype of *FRT*^{79D}*-CycT*^{j11B2} MARCM clones 7 days after clonal induction. (K) The rescued cells by expression of *p35* in *FRT*^{79D}*-CycT*^{j11B2} MARCM clones eventually died 14 days after clonal induction. (L) Control *FRT*^{19A} MARCM clones 14 days after clonal induction. The posterior midguts of corresponding flies were dissected, stained with the indicated antibodies, and analyzed by confocal microscopy. Scale bars, 10 μm.

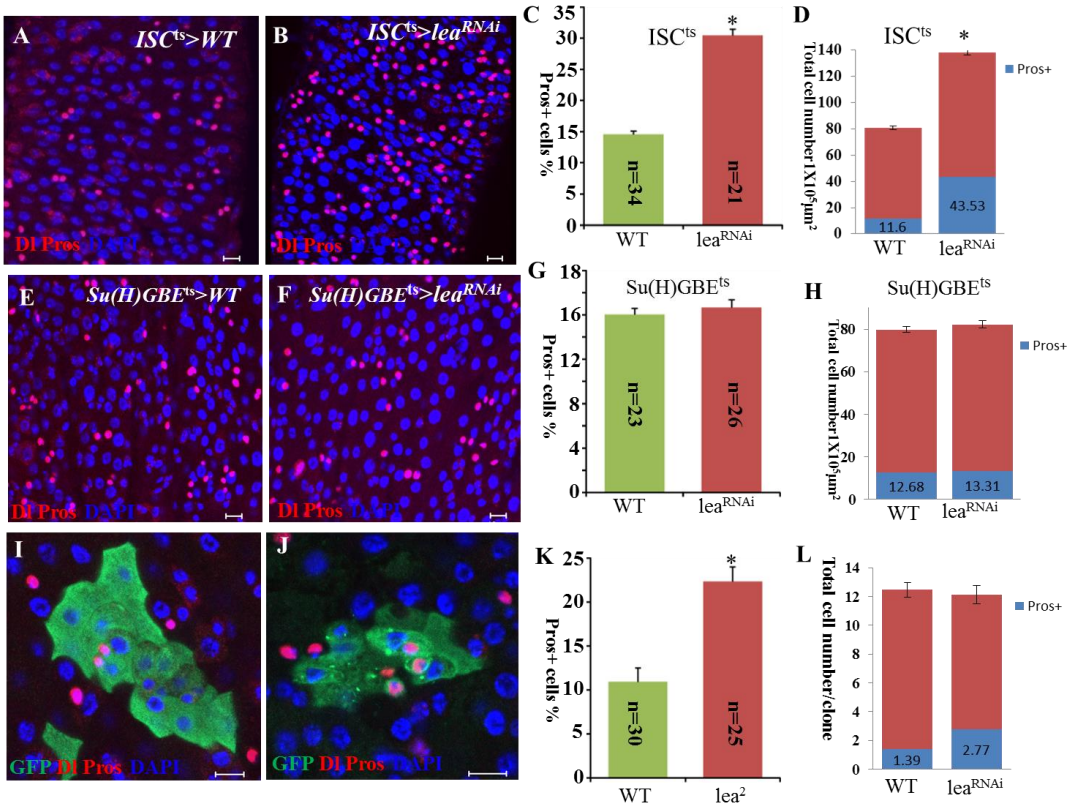

Figure S3, Related to Figure 6. Robo2 Represses EE Cell Generation in ISCs. (A–G) Knockdown of *lea* in ISCs (*ISC*^{ts}*>lea*^{RNAi};B), but not in EBs [*Su(H)GBE*^{ts}*>lea*^{RNAi};F), resulted in a significant increase the percentage of Pros+ EE cells, as compared with their wild-type counterparts (B compares with A; F compares with E). (C) The quantitative percentages of Pros+ cells among all cells in A and B. (D) The quantitative cell numbers (total Pros+ cells in blue box) in equal areas in A and B. (G) The quantitative percentages of Pros+ cells among all cells in E and F. (H) The quantitative cell numbers (total Pros+ cells in blue box) in equal areas in E and F. (I–L) MARCM clones of wild-type control (I) and *lea*^{2} (J). Seven days after clone induction, the proportion of Pros+ EE cells is significantly higher in the GFP-marked clones of both *lea*^{2} (J), as compared with its wild-type counterpart (I), while the clone sizes are similar. (K) The quantitative percentages of Pros+ cells in GFP+ cells in I and J. (L) The quantitative cell numbers (total Pros+ cells in blue box) per clone in I and J. The adult fly posterior midguts were stained with the indicated antibodies. Scale bars, 5 μm.

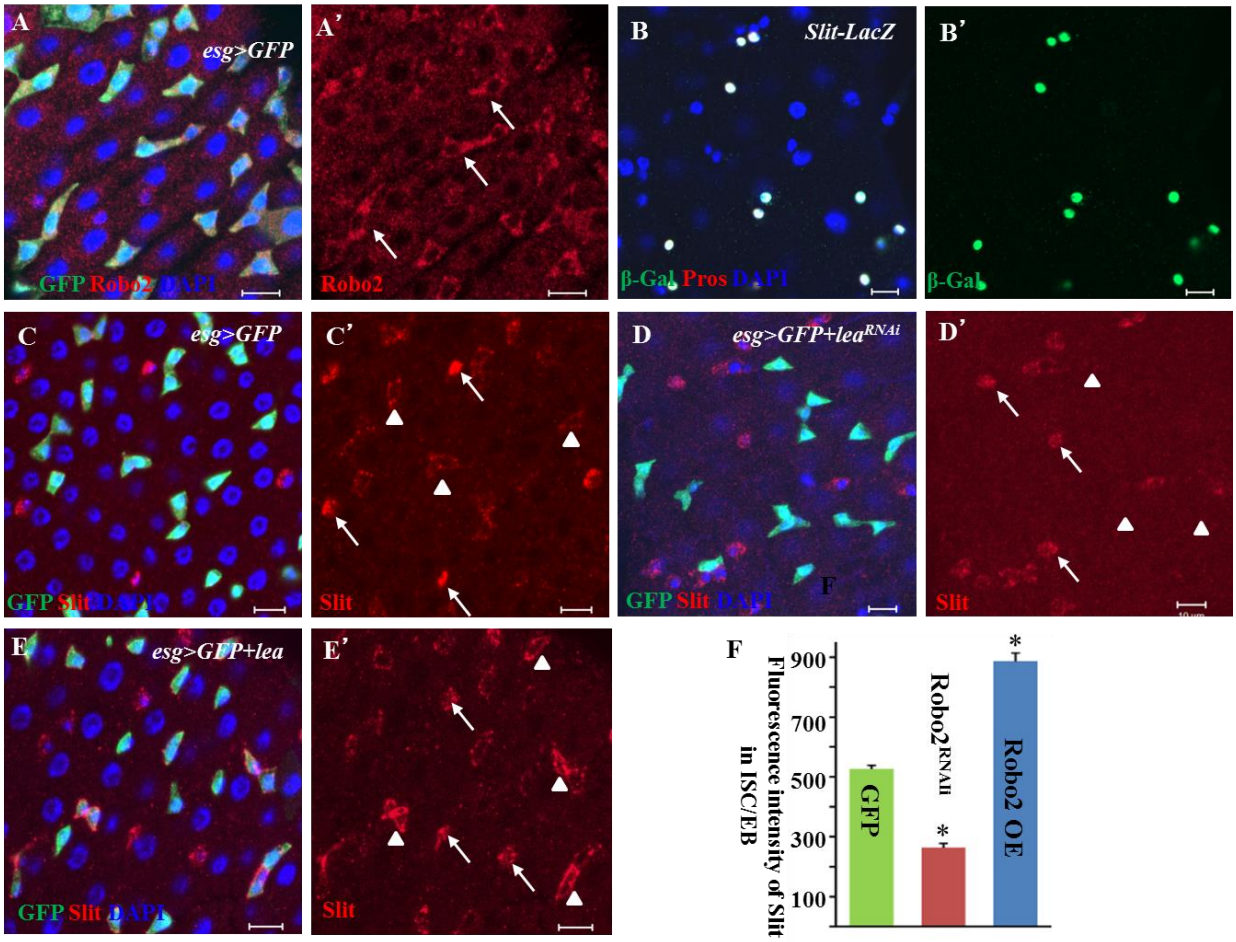

Figure S4, Related to Figure 6. A Slit-Robo2 Signaling from EE cells to ISCs Regulates the Number of EE Cells through a negative feedback mechanism.

(A, A') The Robo2 protein is expressed in mainly Esg-positive ISCs and Ebs (arrows in A'). (B, B') The *slit* gene is expressed mainly in EE cells (as detected by β-galactosidase in the $slit^{PZ05248}$ reporter line). (C, C') The Slit protein is strongly expressed in EE cells (arrows in C') and weakly expressed in the periphery of Esg-positive ISCs and EBs (arrowheads in C'). (D, D') Knockdown of *lea* ($esg^{ts} > lea^{RNAi}$) in ISCs and EBs is sufficient to reduce the amount of Slit protein near the periphery of these cells (arrowheads in D') without affecting its expression in EE cells (arrows in D'). (E, E') Overexpression of *Robo2/lea* ($esg^{ts} > lea^{EP2582}$) in ISCs and EBs is sufficient to increase the accumulation of Slit protein at the periphery of these cells (arrowheads in E') without affecting its expression in EE cells (arrows in E'). (F) Quantitation of Slit protein near the periphery of ISCs and EBs in C–E. Scale bars in all panels, 5 μm.

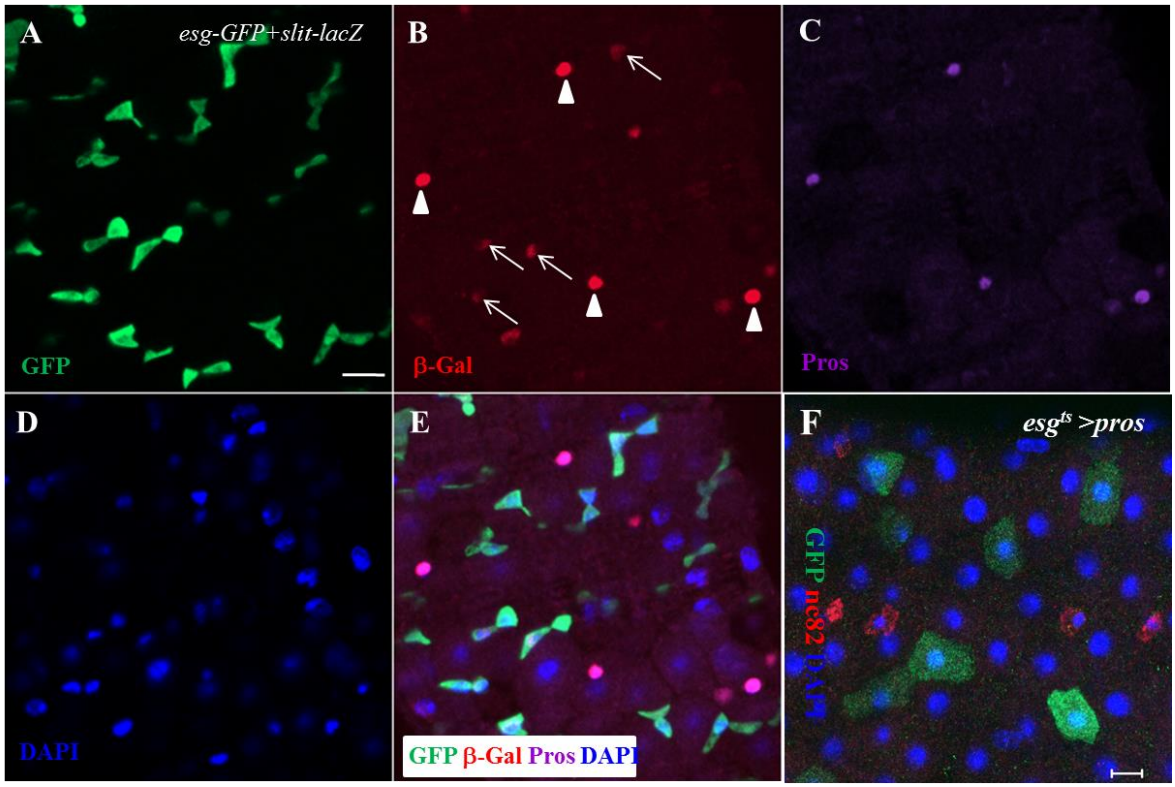

Figure S5, Related to Figure 6. *slit* gene is strongly expressed in EEs and weakly in ISCs.
(A-E) The *slit* gene is strongly expressed in EE cells (arrowheads in B) and weakly in ISCs (arrows in B). (F) Overexpression of *pros* in ISCs (*ISC*^{ts}>*pros*). The adult fly posterior midguts were stained with the indicated antibodies. Scale bars in all panels, 5 μm.

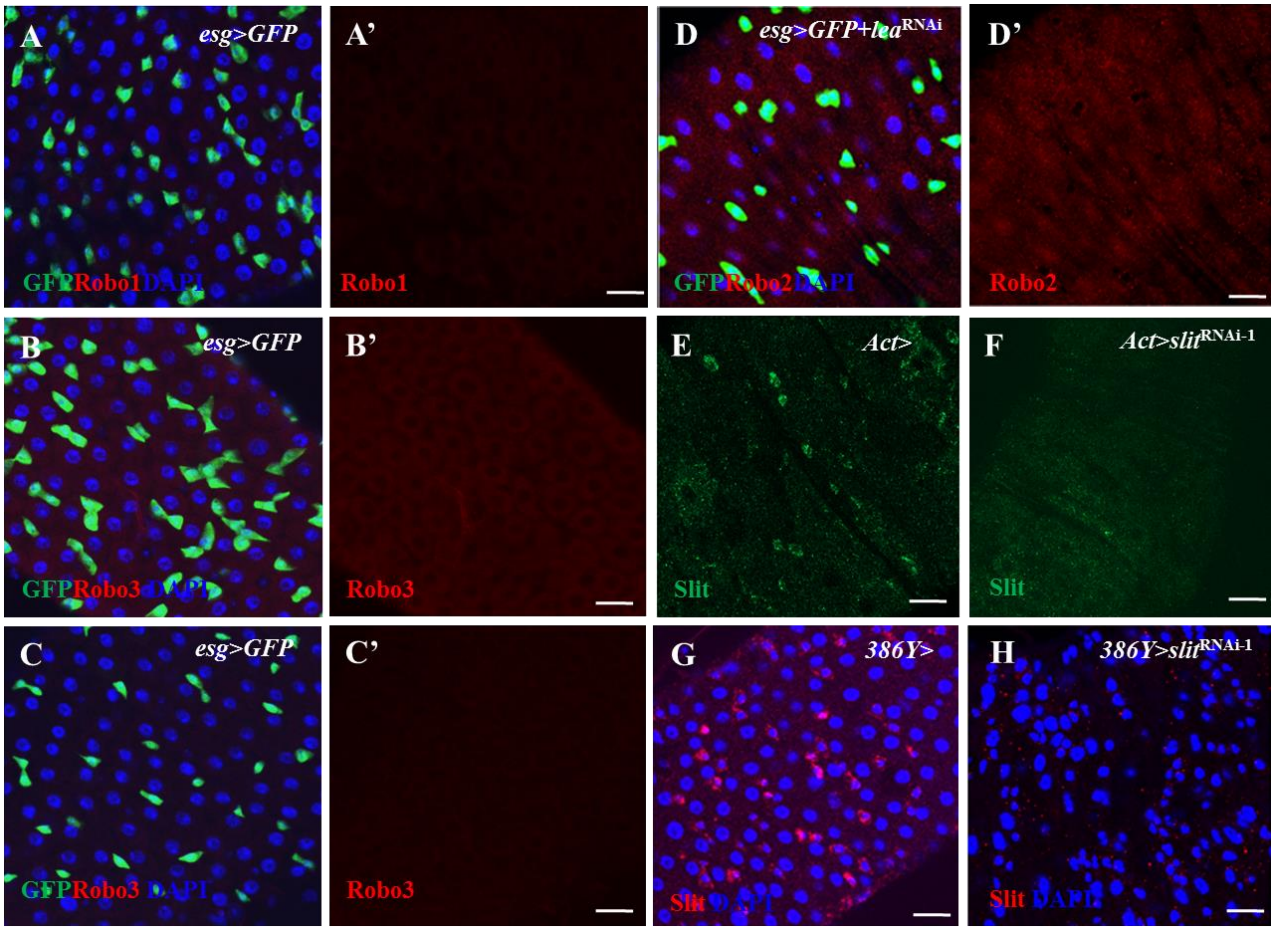

Figure S6, Related to Figure 6. Expression of Robo1 and Robo3 and efficiency of *lea* and *slit* RNAi. (A, A') The Robo1 protein is not detected in posterior midgut. (B-C') The Robo3 protein is not detected in posterior midgut. In B and B', mouse anti-Robo3 cytoplasmic (15H2) antibody was used. In C and C', mouse anti-Robo3 extracellular (14C9) antibody was used. (D, D') The Robo2 protein is effectively reduced in the $esg^{ts}>lea^{RNAi}$ flies. (E, F) The Slit protein is effectively reduced in the $act^{ts}>slit^{RNAi\text{-}1}$ flies. (G, H) The Slit protein is effectively reduced in the *386Y*> $slit^{RNAi\text{-}1}$ flies. The adult fly posterior midguts were stained with the indicated antibodies. Scale bars in all panels, 5 μm.

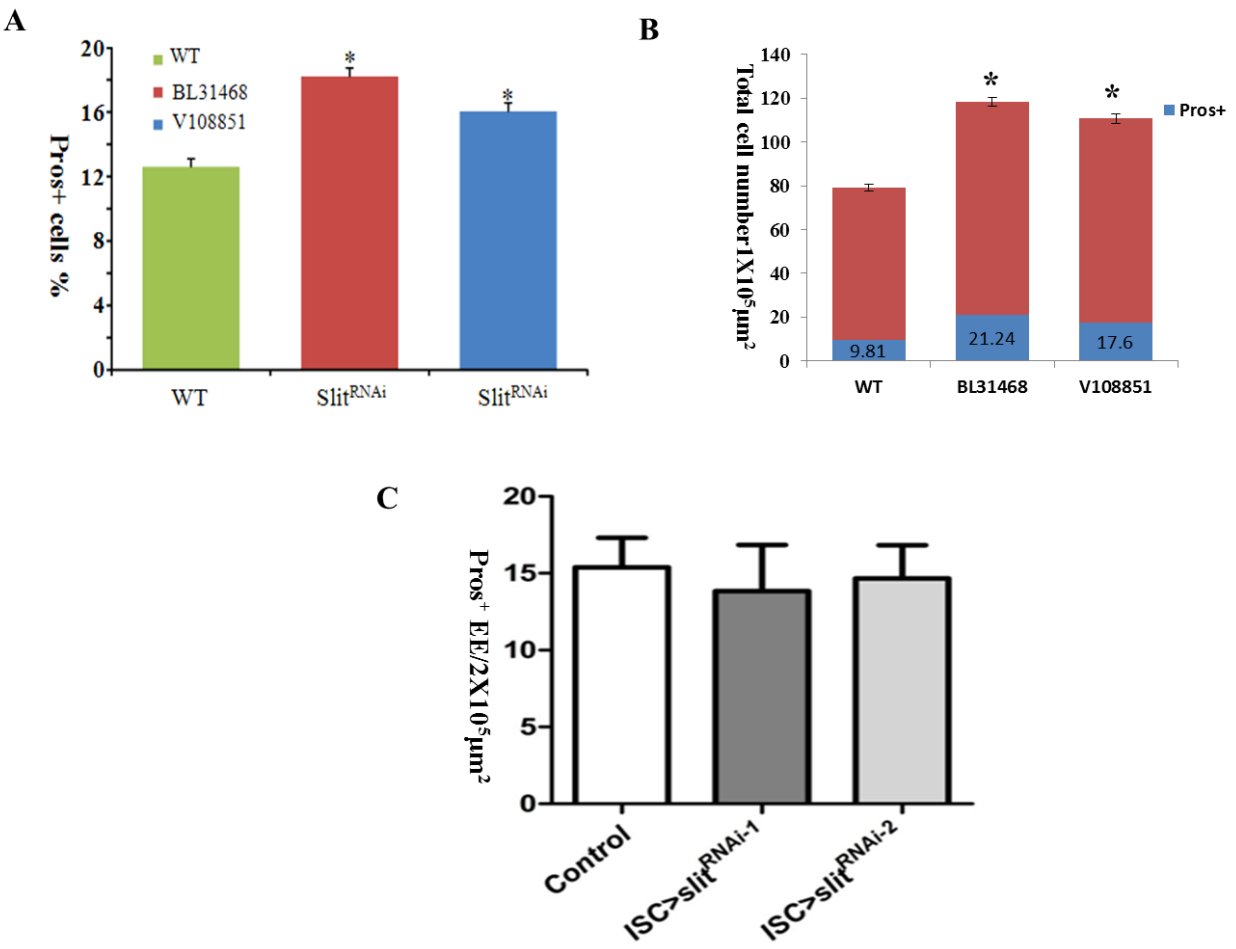

Figure S7. **Related to Figure 6. Knockdowns of *slit* in EEs rather than in ISCs affect EE numbers.** (A) Knockdown of *slit* in EE cells (*386Y>slit*^{RNAi}) resulted in a small but significant increase the number of Pros+ EE cells, as compared with their wild-type counterparts. (B) The quantitative cell numbers (total Pros+ cells in blue box) in equal areas in A and B. (C) Knockdown of *slit* in ISCs (*ISC*^{ts} >*slit*^{RNAi}) did not significantly affect the number of Pros+ EE cells, as compared with their wild-type counterparts. The wild type, *386Y>slit*^{RNAi} , and *ISC*^{ts} >*slit*^{RNAi} flies were stained using anti-Pros antibody after 14 days at 29°C.

SUPPLEMENTAL EXPERIMENTAL PROCEDURES

qPCR.

Total RNA from Act>RNAi adult fly guts was isolated using the RNeasy™ Mini Kit (Qiagen) with on-column DNase digestion to remove genomic DNA. cDNA was synthesized using the ThermoScript™ RT-PCR System (Invitrogen). Real-time PCR analysis was performed on a real-time PCR system, Mastercycler Realplex (Eppendorf), using SYBR Green PCR Master Mix (Clontech). Primers were selected using FlyPrimer Bank.

Bioinformatics analysis.

1. The ISC genetic network (Figure 3A) was generated as previously described in Yan et al 2014. In brief: The network was built by generating an interaction matrix using the following sources: protein-protein interactions (BioGrid, IntAct, MINT, DIP, DPiM and DroID (Sep 2012 version)), genetic interactions (FlyBase, BioGrid and DroID (Sep 2012 version)) and Literature cocitation interactions: gene2pubmed association was retrieved from NCBI EntrezGene ftp site (ftp://ftp.ncbi.nlm.nih.gov/gene/DATA/) on Jan 8th 2013. Pairwise gene co- citation relationships were extracted from PubMed. An interaction matrix was established amongst all genes that scored in the ISC screen and the resulting network was visualized using the Cytoscape software. Molecular complexes or groups of genes with the same function are outlined in black. Note: Genes that are not part of the interaction network are not displayed in the Figure.

2. Complex analysis: Complex analysis was done using COMPLEAT (http://www.flyrnai.org/compleat/), a tool that annotates protein complexes from both literature and predictions from protein-protein network, and does gene set enrichment analysis based on protein complexes. Using COMPLEAT, we identified 79 non-redundant protein complexes that are over-represented among the genes scored comparing to the experimental background with p value cut-off 0.05 (Table S3).

3. ISC, Nb, and female GSC comparison (Figure 7B) and GO enrichment heatmap (Figure 7A).

GO term enrichment was performed with DAVID (http://david.abcc.ncifcrf.gov) for ISC, GSC and Nb screens.